

Synthesis and Properties of $[(\eta\text{-C}_5\text{H}_5)\text{Re}(\text{NO})(\text{PPh}_3)(=\text{CHC}_6\text{H}_5)]^+\text{PF}_6^-$: A Benzylidene Complex That Is Formed by a Stereospecific α -Hydride Abstraction, Exists as Two Geometric Isomers, and Undergoes Stereospecific Nucleophilic Attack

William A. Kiel,^{1a} Gong-Yu Lin,^{1a} Anthony G. Constable,^{1a} Fred B. McCormick,^{1a}
 Charles E. Strouse,^{1a} Odile Eisenstein,^{*1b,2} and J. A. Gladysz^{*1a,3}

Contribution from the Departments of Chemistry, University of California, Los Angeles,
 California 90024, and University of Michigan, Ann Arbor, Michigan 48109.

Received February 26, 1982

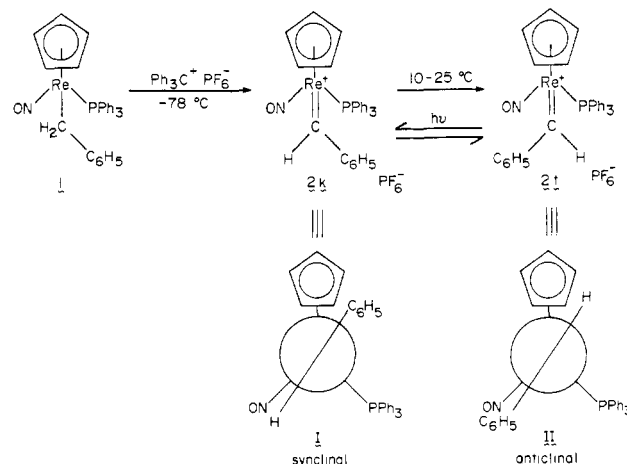
Abstract: Reaction of $(\eta\text{-C}_5\text{H}_5)\text{Re}(\text{NO})(\text{PPh}_3)(\text{CH}_2\text{C}_6\text{H}_5)$ (**1**) with $\text{Ph}_3\text{C}^+\text{PF}_6^-$ at -78°C gives the benzylidene *sc*- $[(\eta\text{-C}_5\text{H}_5)\text{Re}(\text{NO})(\text{PPh}_3)(=\text{CHC}_6\text{H}_5)]^+\text{PF}_6^-$ (**2k**), which isomerizes upon warming ($t_{1/2} = 17$ min at 29.5°C , $\Delta H^\ddagger = 20.9 \pm 0.4$ kcal/mol, $\Delta S^\ddagger = -3.8 \pm 0.2$ eu) to a new $\text{Re}=\text{C}$ geometric isomer, *ac*- $[(\eta\text{-C}_5\text{H}_5)\text{Re}(\text{NO})(\text{PPh}_3)(=\text{CHC}_6\text{H}_5)]^+\text{PF}_6^-$ (**2t**). The **2t/2k** equilibrium mixture is $\geq 99:1$, but irradiation between -78 and -20°C establishes a $(55 \pm 3):(45 \pm 3)$ photostationary state. The structures of **2t** and **2k** are confirmed by X-ray crystallography (**2t**) and extended Hückel MO calculations. Nucleophiles (Nu) $\text{Li}(\text{C}_2\text{H}_5)_3\text{BD}$, CH_3Li , $\text{CH}_3\text{CH}_2\text{MgBr}$, $\text{C}_6\text{H}_5\text{CH}_2\text{MgCl}$, PMe_3 , and CH_3ONa attack **2t** to give diastereomerically pure adducts $(\eta\text{-C}_5\text{H}_5)\text{Re}(\text{NO})(\text{PPh}_3)(\text{CHNuC}_6\text{H}_5)$, in which a new chiral center is stereospecifically generated. The same nucleophiles react stereoselectively with **2k**, affording adducts in (generally) 92–95:8–5 diastereomer ratios. The minor diastereomers from **2k** are identical with the products from **2t**. Thus nucleophilic attack upon **2t** and **2k** occurs preferentially from the same direction. An X-ray structure of $(SS,RR)\text{-}(\eta\text{-C}_5\text{H}_5)\text{Re}(\text{NO})(\text{PPh}_3)(\text{CH}(\text{CH}_2\text{C}_6\text{H}_5)\text{C}_6\text{H}_5)$ (**5t**, from $\text{C}_6\text{H}_5\text{CH}_2\text{MgCl}$ attack upon **2t**) establishes this direction to be antiperiplanar to the PPh_3 . When $(SS,RR)\text{-}(\eta\text{-C}_5\text{H}_5)\text{Re}(\text{NO})(\text{PPh}_3)(\text{CHDC}_6\text{H}_5)$ (**1- α -d₁-t**; from $\text{Li}(\text{C}_2\text{H}_5)_3\text{BD}$ attack upon **2t**) is treated with $\text{Ph}_3\text{C}^+\text{PF}_6^-$, exclusive H^- abstraction occurs to give first **2k- α -d₁** and then **2t- α -d₁**. When $(SR,RS)\text{-}(\eta\text{-C}_5\text{H}_5)\text{Re}(\text{NO})(\text{PPh}_3)(\text{CHDC}_6\text{H}_5)$ (**1- α -d₁-k**; from $\text{Li}(\text{C}_2\text{H}_5)_3\text{BH}$ attack upon **2t- α -d₁** or $\text{Li}(\text{C}_2\text{H}_5)_3\text{BD}$ attack upon **2k**) is treated with $\text{Ph}_3\text{C}^+\text{PF}_6^-$, preferential (92:8) D^- abstraction occurs to give undeuterated **2k** and (subsequently) **2t**. These data (after an isotope effect correction) indicate that the *pro-R* α -hydrogen of **1** is abstracted by $\text{Ph}_3\text{C}^+\text{PF}_6^-$ essentially stereospecifically. Insights into this specificity are gained by ^1H NMR, extended Hückel MO calculations, and the chemospecific and stereospecific abstraction of CH_3O^- from $(\eta\text{-C}_5\text{H}_5)\text{Re}(\text{NO})(\text{PPh}_3)(\text{CH}(\text{OCH}_3)\text{C}_6\text{H}_5)$ (**SR,RS**: **7t**; **SS,RR**: **7k**) by $\text{Ph}_3\text{C}^+\text{PF}_6^-$. A mechanism is proposed in which the least stable rotamer of **1** is the most reactive toward $\text{Ph}_3\text{C}^+\text{PF}_6^-$.

Introduction

During the last decade, the use of chiral transition-metal catalysts in asymmetric organic synthesis has received increasing attention.⁴ Extremely useful *stoichiometric* reagents such as Sharpless' $\text{Ti}(\text{O-}i\text{-Pr})_4/t\text{-BuOOH}$ /diethyl tartrate system for asymmetric epoxidation have also been developed.⁵ However, understanding of the mechanistic basis for chirality transfer is still at a very formative stage. Some surprising results have been obtained from initial studies. For instance, the $[\text{Rh}(\text{S,S-chiraphos})\text{S}_2]^+$ -catalyzed⁶ asymmetric hydrogenation of prochiral enamides proceeds via the *less* stable of two diastereomeric olefin complexes.

We recently described syntheses of rhenium alkyls and alkylidenes of the formulas $(\eta\text{-C}_5\text{H}_5)\text{Re}(\text{NO})(\text{PPh}_3)(\text{CH}_2\text{R})$ and $[(\eta\text{-C}_5\text{H}_5)\text{Re}(\text{NO})(\text{PPh}_3)(=\text{CHR})]^+\text{PF}_6^-$.⁷ Both classes of compounds contain a pseudotetrahedral asymmetric rhenium and have been found to undergo unprecedented ligand-based stereospecific (or highly stereoselective) stoichiometric reactions. These transformations offer the opportunity to study the transfer of metal-centered chirality to carbon at a fundamental level and consequently have been the subject of detailed investigations in our laboratory.

Scheme I. Syntheses and Interconversions of Isomeric Benzylidene Complexes¹⁰



In this paper, we present a full account of our work with the benzyl complex $(\eta\text{-C}_5\text{H}_5)\text{Re}(\text{NO})(\text{PPh}_3)(\text{CH}_2\text{C}_6\text{H}_5)$ (**1**) and the benzylidene complex $[(\eta\text{-C}_5\text{H}_5)\text{Re}(\text{NO})(\text{PPh}_3)(=\text{CHC}_6\text{H}_5)]^+\text{PF}_6^-$ (**2**).⁷⁻⁹ As will be disclosed, three principal findings emerge from our *chemical* data:

(a) Reaction of $(\eta\text{-C}_5\text{H}_5)\text{Re}(\text{NO})(\text{PPh}_3)(\text{CH}_2\text{C}_6\text{H}_5)$ (**1**) with $\text{Ph}_3\text{C}^+\text{PF}_6^-$ results in abstraction of only one of the two diastereotopic α hydrogens.

(b) The product from a, benzylidene **2**, is generated initially as a "kinetic" $\text{Re}=\text{C}$ geometric isomer (**2k**); at $10\text{--}25^\circ\text{C}$, **2k** isomerizes to a "thermodynamic" geometric isomer (**2t**).

(8) Constable, A. G.; Gladysz, J. A. *J. Organomet. Chem.* **1980**, 202, C21.

(9) McCormick, F. B.; Kiel, W. A.; Gladysz, J. A. *Organometallics* **1982**, 1, 405.

(1) (a) UCLA. (b) University of Michigan.

(2) Address all correspondence on the MO calculations to this author.

(3) Address other correspondence to this author at the Department of Chemistry, University of Utah, Salt Lake City, UT 84112; Fellow of the Alfred P. Sloan Foundation (1980–1984) and Camille and Henry Dreyfus Teacher-Scholar Grant Recipient (1980–1985).

(4) (a) Kagan, H. B.; Fiund, J. C. *Top. Stereochem.* **1978**, 10, 175. (b) Fryzuk, M. D.; Bosnich, B. *J. Am. Chem. Soc.* **1979**, 101, 3043. (c) Valentine, D., Jr.; Scott, J. W. *Synthesis* **1978**, 329.

(5) Katsuki, T.; Sharpless, K. B. *J. Am. Chem. Soc.* **1980**, 102, 5974.

(6) Chan, A. S. C.; Pluth, J. J.; Halpern, J. *J. Am. Chem. Soc.* **1980**, 102, 5952. Chua, P. S.; Roberts, N. K.; Bosnich, B.; Okrasinski, S. J.; Halpern, J. *J. Chem. Soc., Chem. Commun.* **1982**, 1278. Chiraphos = $(SS,RR)\text{-}(\text{C}_6\text{H}_5)_2\text{PCH}(\text{CH}_3)\text{CH}(\text{CH}_3)\text{P}(\text{C}_6\text{H}_5)_2$.

(7) Kiel, W. A.; Lin, G.-Y.; Gladysz, J. A. *J. Am. Chem. Soc.* **1980**, 102, 3299.

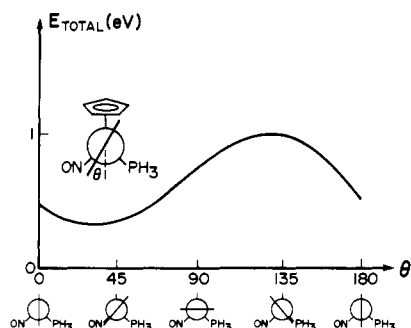


Figure 1. Calculated E_{total} for $[(\eta\text{-C}_5\text{H}_5)\text{Re}(\text{NO})(\text{PPh}_3)(=\text{CH}_2)]^+$ as the $=\text{CH}_2$ ligand is rotated.

(c) Benzylidenes **2k** and **2t** undergo stereoselective and stereospecific attack, respectively, when treated with a variety of nucleophiles.

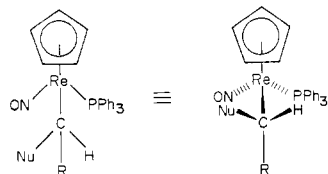
We then describe the use of physical and theoretical methods (two X-ray crystal structures; extended Hückel MO calculations) to precisely define the stereochemical relationships between the starting materials and products in a–c and to provide insight into the origins of stereocontrol.

Results

1. Synthesis and Structural Characterization of Benzylidene Complexes. The benzyl complex $(\eta\text{-C}_5\text{H}_5)\text{Re}(\text{NO})(\text{PPh}_3)(\text{CH}_2\text{C}_6\text{H}_5)$ (**1**) was treated with 1.1 equiv of $\text{Ph}_3\text{C}^+\text{PF}_6^-$ in CD_2Cl_2 at -78°C . Proton NMR monitoring (-70°C) indicated the clean and immediate formation of a cationic benzylidene complex (**2k**; Scheme I),¹⁰ as evidenced by a characteristic¹¹ low-field $\text{Re}=\text{CH}(\text{C}_6\text{H}_5)$ resonance (δ 16.08 (s, 1 H)) and a deshielded C_5H_5 resonance (δ 5.89 (s, 5 H)). When this solution was warmed to $10\text{--}25^\circ\text{C}$, **2k** began to disappear as a new benzylidene complex, **2t**, formed (δ 15.30 (s, 1 H), 6.06 (s, 5 H)). At room temperature, the equilibrium ratio of **2t/2k** was $>99:1$. After solvent removal and recrystallization, **2t** was isolated in 73–75% yields as yellow, air-stable powder or crystals (Experimental Section) which were stable to $>200^\circ\text{C}$. Attempts to isolate **2k** by low-temperature crystallization gave only impure oils.

Additional experiments indicated **2k** and **2t** to be geometric isomers differing in the orientation of ligands about the $\text{Re}=\text{C}$ double bond. First, both **2k**¹² and **2t** reacted cleanly with $\text{Li}(\text{C}_2\text{H}_5)_3\text{BH}$ to give **1**. This transformation established the benzylidene carbon to be electrophilic. Second, irradiation of CD_2Cl_2 , CD_3CN , or $(\text{CD}_3)_2\text{CO}$ solutions of **2t** (Hanovia 450-W lamp, through Pyrex) between -78 and -20°C afforded, after 3 h, clean (55 \pm 3):(45 \pm 3) photostationary states of **2t** and **2k**, as determined by ^1H NMR integration of the C_5H_5 resonances. These solutions were allowed to return to thermal equilibrium in the dark. A sample to which *p*-di-*tert*-butylbenzene had been added indicated $>95\%$ of the original **2t** to be present. Thus **2t** and **2k** can be photointerconverted analogously to $\text{C}=\text{C}$ double-bond geometric isomers.^{9,13}

(10) For the conversion of planar representations of rhenium complexes into three dimensional structures, we employ the convention shown in Scheme I for alkylidenes⁸ and the following convention for alkyls:



(11) Brookhart, M.; Nelson, G. O. *J. Am. Chem. Soc.* **1977**, *99*, 6099.

(12) Unless otherwise noted, reactions of **2k** were conducted with material prepared in situ at -78°C .

(13) (a) Saltiel, J.; D'Agostino, J.; Megarity, E. D.; Metts, L.; Neuberger, K. R.; Wrighton, M.; Zafirou, O. C. In "Organic Photochemistry"; Chapman, O. L., Ed.; Marcel Dekker: New York, 1973; Vol. 3, pp 1–113. (b) Saltiel, J.; Charlton, J. L. In "Rearrangements in Ground Excited States"; de Mayo, P., Ed.; Academic Press: New York, 1980; Vol. 3, p 25.



Figure 2. Stereoview of the molecular structure of $ac\text{-}[(\eta\text{-C}_5\text{H}_5)\text{Re}(\text{NO})(\text{PPh}_3)(=\text{CHC}_6\text{H}_5)]^+\text{PF}_6^-\cdot\text{CHCl}_3$ (**2t**· CHCl_3).

Table I. Selected Bond Lengths and Bond Angles in **2t**· CHCl_3

atoms	dist, Å	atoms	angle, deg
Re–C1	1.949 (6)	Re–C1–C21	136.2 (5)
Re–P1	2.427 (2)	Re–C1–H1	117 ^b
Re–N	1.761 (5)	N–Re–C1	99.8 (2)
Re–C ₅ H ₅ ^a	2.333	P1–Re–N	91.0 (2)
N–O1	1.195 (7)	P1–Re–C1	93.2 (2)
C1–H1	0.98 ^b	O1–N–Re	172.7 (5)
C1–C21	1.454 (9)		

^a Average distance from Re to C_5H_5 carbons. ^b H1 was not refined.

Since geometric isomerism due to metal–carbon multiple bonding was without precedent, we turned to an MO analysis for additional insight. Extended Hückel MO calculations have been previously shown to accurately predict metal–alkylidene bonding geometries.¹⁴ Computations on the parent model system¹⁵ $[(\eta\text{-C}_5\text{H}_5)\text{Re}(\text{NO})(\text{PPh}_3)(=\text{CH}_2)]^+$ showed two degenerate energy minima, separated by a $\sim 19\text{-kcal}$ barrier, as the rhenium–methylidene bond was rotated through 360° (Figure 1). In the favored conformer, the $=\text{CH}_2$ plane eclipsed the (C)Re–N–O plane. Thus two *nondegenerate* minima, I and II (Scheme I; Newman projections down the benzylidene–rhenium bond) are expected as the benzylidene ligand in **2** is rotated through 360° .

Space-filling molecular models indicated II to be considerably less congested than I. In the former, the benzylidene phenyl ring eclipses the small NO ligand, whereas in the latter it is forced to reside between the bulky PPh_3 and medium-sized C_5H_5 ligand. Calculations on the model system $[(\eta\text{-C}_5\text{H}_5)\text{Re}(\text{NO})(\text{PPh}_3)(=\text{CHC}_6\text{H}_5)]^+$ indicated II to be more stable than I as long as the benzylidene phenyl ring was canted at least 25° with respect to the (C)Re–N–O plane (i.e., slightly out of conjugation with $\text{Re}=\text{C}$). This relieves a repulsive nonbonding interaction between the NO and an ortho proton of the benzylidene phenyl ring.

A definitive structural assignment for **2t** was made by X-ray crystallography. A suitable single crystal ($0.19 \times 0.20 \times 0.30$ mm; CHCl_3 monosolvate) was obtained by slow diffusion of petroleum ether (bp $30\text{--}60^\circ\text{C}$) into a CHCl_3 solution of **2t**. X-ray data were obtained at -158°C by using monochromated $\text{Mo K}\alpha$ (0.71069 Å) radiation on a Syntex P1 automatic diffractometer. The general techniques employed have been previously described.¹⁶ The unit cell was found to be triclinic, space group $P\bar{1}$ ($Z = 2$), with lattice parameters $a = 8.984$ (5) Å, $b = 14.008$ (6) Å, $c = 13.965$ (7) Å, $\alpha = 109.06$ (4) $^\circ$, $\beta = 101.92$ (4) $^\circ$, $\gamma = 75.99$ (4) $^\circ$. Of 5666 reflections with $2\theta < 50^\circ$ collected, 5070 with $I \geq 3\sigma(I)$ were used in the final refinement. The positions of the Re and P(1) atoms were obtained from a three-dimensional Patterson map. Several least-squares refinements yielded all non-hydrogen atoms, including the CHCl_3 , in the unit cell. Absorption corrections were then applied after which all hydrogens were located from a difference Fourier map. The rhenium, chlorine, fluorine, and

(14) (a) Schilling, B. E. R.; Hoffmann, R.; Faller, J. W. *J. Am. Chem. Soc.* **1979**, *101*, 592. (b) Schilling, B. E. R.; Hoffmann, R.; Lichtenberger, D. L. *Ibid.* **1979**, *101*, 585.

(15) (a) The isolation of the methylidene complex $[(\eta\text{-C}_5\text{H}_5)\text{Re}(\text{NO})(\text{PPh}_3)(=\text{CH}_2)]^+\text{PF}_6^-$ has been described in a separate publication.^{15b} (b) Tam, W.; Lin, G.-Y.; Wong, W. K.; Kiel, W. A.; Wong, V. K.; Gladysz, J. A. *J. Am. Chem. Soc.* **1982**, *104*, 141.

(16) Strouse, J.; Layten, S. W.; Strouse, C. E. *J. Am. Chem. Soc.* **1977**, *99*, 562.

Table II. Rate Constants for the Re=C Bond Rotation $2\mathbf{k} \rightarrow 2\mathbf{t}$ in CD_2Cl_2 ^a

entry	temp (± 0.1 °C)	$10^5 k_{\text{obsd}}, \text{s}^{-1}$
1	29.5	69.2 ± 0.6
2	24.0	37.6 ± 0.6
3	19.0	20.5 ± 0.2
4	19.0	19.2 ± 0.2
5 ^b	19.0	20.9 ± 0.3
6	14.0	11.5 ± 0.2
7	10.0	4.81 ± 0.10
8	10.0	6.93 ± 0.10
9	4.0	2.61 ± 0.03

^a $[2\mathbf{k}]_0 = 0.038 - 0.042$ M. Entries 1–5 were followed through $>2t_{1/2}$; others were followed through at least one $t_{1/2}$. See Experimental Section for further details. ^b $2\mathbf{k}$ photochemically generated at -78 °C.

phosphorus atoms were refined with anisotropic temperature factors, and all other non-hydrogen atoms were refined with isotropic thermal parameters. All hydrogen atoms were held at positions indicated from the map with assigned isotropic thermal parameters. The final R index was 0.039 with $R_w = 0.049$.¹⁷

The molecular structure of $2\mathbf{t} \cdot \text{CHCl}_3$ thus obtained is shown in Figure 2. The near eclipsing of the (C1)Re–N–O1 and H1–C1–C21 planes (torsion angle = $4.0 \pm 0.7^\circ$) is evident. Thus $2\mathbf{t}$ has the structure approximated by Newman projection II (Scheme I). Since the MO calculations indicate only two energy minima as rhenium–alkylidene bonds are rotated through 360° , $2\mathbf{k}$ can confidently be assigned the structure I.

An exhaustive list of bond distances and angles in $2\mathbf{t} \cdot \text{CHCl}_3$ and a crystal packing diagram are provided in the supplementary material. Important bond distances and angles are summarized in Table I. The P1–Re–N angle of 91.0 (2°) is expected based upon crystal structures of other, formally octahedral, $(\eta\text{-C}_5\text{H}_5)\text{ML}_3$ ($M = \text{Mn}, \text{Re}$) complexes.^{18a} Hence the corresponding angles in Newman projections I–XIV (normally 120°) have been compressed. As anticipated by the calculations, the least-squares plane of the benzylidene phenyl ring (Figure 2) is canted $19.9 \pm 0.8^\circ$ with respect to the Re=C vector.

Benzylidene complexes $2\mathbf{k}$ and $2\mathbf{t}$ were further characterized by isomerization rate measurements and UV–visible spectroscopy. The first-order rate constant for equilibration of a $(55 \pm 3):(45 \pm 3)$ $2\mathbf{t}/2\mathbf{k}$ photostationary state (in CD_2Cl_2) back to $2\mathbf{t}$ was measured by ^1H NMR at 19 °C (entry 5, Table II). The k_{obsd} obtained was in good agreement with the k_{obsd} determined (19 °C) from $2\mathbf{k}$ prepared in situ from $(\eta\text{-C}_5\text{H}_5)\text{Re}(\text{NO})(\text{PPh}_3)(\text{CH}_2\text{C}_6\text{H}_5)$ and $\text{Ph}_3\text{C}^+\text{PF}_6^-$ (entries 3 and 4, Table II). Hence, data obtained by the latter route can reliably be used to calculate activation parameters for rotation about rhenium–alkylidene bonds. Rate constants for $2\mathbf{k} \rightarrow 2\mathbf{t}$ were measured from 4 °C ($t_{1/2} = 443$ min) to 29.5 °C ($t_{1/2} = 17$ min), as summarized in Table II. These yielded $\Delta H^\ddagger = 20.9 \pm 0.4$ kcal/mol and $\Delta S^\ddagger = -3.8 \pm 0.2$ eu.^{18b}

The absorption spectrum of $2\mathbf{t}$ displayed a λ_{max} at 365 nm (ϵ 13 000) in CH_3CN . A series of spectra (Figure 3) were recorded as a CH_2Cl_2 $2\mathbf{t}/2\mathbf{k}$ photostationary state was warmed from -78 °C to room temperature. An isosbestic point was evident as $2\mathbf{k}$ isomerized to $2\mathbf{t}$. Its location indicates that λ_{max} for $2\mathbf{k}$ is at a shorter wavelength than for $2\mathbf{t}$.

2. Stereochemistry of Nucleophilic Attack at Benzylidene Carbon. The exclusive formation of the less stable geometric

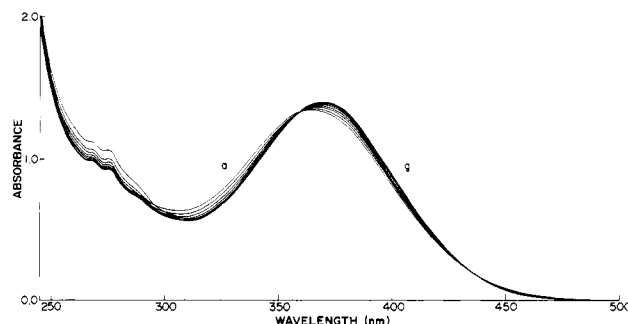


Figure 3. Absorption spectra recorded as a $(55 \pm 3):(45 \pm 3)$ $2\mathbf{t}/2\mathbf{k}$ mixture in CH_2Cl_2 (prepared by photolysis at -78 °C) was warmed to room temperature: initial spectrum, trace a; final spectrum, trace g.

isomer $2\mathbf{k}$ upon reaction of $\mathbf{1}$ with $\text{Ph}_3\text{C}^+\text{PF}_6^-$ suggested to us that only one of the two diastereotopic α -hydrides underwent abstraction. The widely separated α -hydride ^1H NMR chemical shifts, δ 3.50 and 2.89 (CDCl_3 ; couplings: Table V), also hinted at the possibility of differential reactivity. Testing of this hypothesis required the synthesis of $\mathbf{1}$ with an α -deuterium label at either the *pro-R* or *pro-S* site. Obvious routes to such a substrate did not exist, so exploratory reactions of $2\mathbf{k}$ and $2\mathbf{t}$ with nucleophiles were conducted.

Benzylidene $2\mathbf{t}$ was reacted with $\text{Li}(\text{C}_2\text{H}_5)_3\text{BD}$. Subsequently isolated was $1\text{-}\alpha\text{-d}_1\text{-t}$ (92% yield), a compound with two chiral centers (see step a, Scheme III). The ^1H NMR spectrum of $1\text{-}\alpha\text{-d}_1\text{-t}$ in CD_2Cl_2 (δ 3.41 (br d, $J_{\text{H-}^{31}\text{P}} = 8$ Hz, $J_{\text{H-H}} \leq 2$ Hz)) indicated that one of the two diastereotopic hydrogens normally present in $\mathbf{1}$ was completely absent. Hence the addition of D^- to $2\mathbf{t}$ occurred *stereoselectively* on one benzylidene face. As little as 1% of the other possible diastereomer would have been detected.

Authentic samples of the other $1\text{-}\alpha\text{-d}_1$ diastereomer, $1\text{-}\alpha\text{-d}_1\text{-k}$, were available by reaction of $\text{Li}(\text{C}_2\text{H}_5)_3\text{BD}$ with $2\mathbf{k}$.¹² Reaction in this case was *stereoselective*; a $(92 \pm 1):(8 \pm 1)$ mixture of $1\text{-}\alpha\text{-d}_1\text{-k}/1\text{-}\alpha\text{-d}_1\text{-t}$ was obtained. The ^1H NMR monitored reaction of $2\mathbf{k}$ with $\text{Li}(\text{C}_2\text{H}_5)_3\text{BD}$ was complete within 3 min at -73 °C. Since the rate constants in Table II indicate that no $2\mathbf{k} \rightarrow 2\mathbf{t}$ isomerization occurs on this time scale, the lack of stereospecificity must be ascribed to a small amount of $\text{Li}(\text{C}_2\text{H}_5)_3\text{BD}$ attack upon a second benzylidene face of $2\mathbf{k}$.

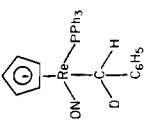
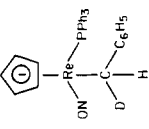
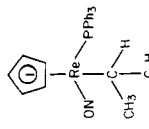
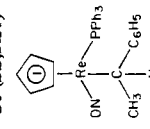
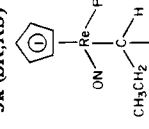
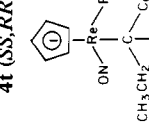
The possibility of crystallographically determining the direction of $\text{Li}(\text{C}_2\text{H}_5)_3\text{BD}$ attack upon $2\mathbf{t}$ was considered. However, a neutron diffraction structure is required to distinguish H from D, and sufficiently large crystals of $1\text{-}\alpha\text{-d}_1\text{-t}$ could not be grown. Fortunately, $2\mathbf{t}$ underwent similar stereospecific attack (as assayed by ^1H NMR spectroscopy of the reaction mixtures prior to any crystallizations) with nucleophiles CH_3Li , $\text{CH}_3\text{CH}_2\text{MgBr}$, $\text{C}_6\text{H}_5\text{CH}_2\text{MgCl}$, PMe_3 , and CH_3ONa . Diastereomerically pure adducts $(\eta\text{-C}_5\text{H}_5)\text{Re}(\text{NO})(\text{PPh}_3)(\text{CH}(\text{CH}_3)\text{C}_6\text{H}_5)$ ($3\mathbf{t}$), $(\eta\text{-C}_5\text{H}_5)\text{Re}(\text{NO})(\text{PPh}_3)(\text{CH}(\text{CH}_2\text{CH}_3)\text{C}_6\text{H}_5)$ ($4\mathbf{t}$), $(\eta\text{-C}_5\text{H}_5)\text{Re}(\text{NO})(\text{PPh}_3)(\text{CH}(\text{CH}_2\text{C}_6\text{H}_5)\text{C}_6\text{H}_5)$ ($5\mathbf{t}$), $[(\eta\text{-C}_5\text{H}_5)\text{Re}(\text{NO})(\text{PPh}_3)(\text{CH}(\text{PMe}_3)\text{C}_6\text{H}_5)]^+\text{PF}_6^-$ ($6\mathbf{t}$), and $(\eta\text{-C}_5\text{H}_5)\text{Re}(\text{NO})(\text{PPh}_3)(\text{CH}(\text{OCH}_3)\text{C}_6\text{H}_5)$ ($7\mathbf{t}$) were subsequently isolated in 75–90% yields. Benzylidene isomer $2\mathbf{k}$ was *stereoselectively* attacked by these nucleophiles.¹² The predominantly formed diastereomer ($3\mathbf{k}\text{--}7\mathbf{k}$) was in each case *opposite* to the one obtained from $2\mathbf{t}$. Diastereomer ratios were assayed by ^1H NMR spectroscopy in situ and/or prior to any workup crystallizations: $3\mathbf{k}/3\mathbf{t}$, $(94 \pm 1):(6 \pm 1)$; $4\mathbf{k}/4\mathbf{t}$, $(95 \pm 1):(5 \pm 1)$; $5\mathbf{k}/5\mathbf{t}$, $(94 \pm 1):(6 \pm 1)$; $6\mathbf{k}/6\mathbf{t}$, $(94 \pm 1):(6 \pm 1)$; $7\mathbf{k}/7\mathbf{t}$, $(78\text{--}85):(22\text{--}15)$. Complexes $3\mathbf{k}\text{--}7\mathbf{k}$ could be obtained in pure form by fractional crystallization. Spectroscopic properties of $3\text{--}7$ are summarized in Table III.

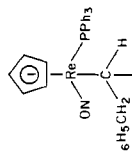
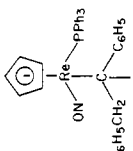
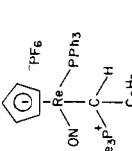
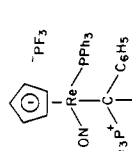
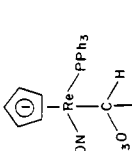
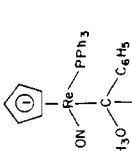
The preceding data constitute compelling evidence that $\text{Li}(\text{C}_2\text{H}_5)_3\text{BD}$, CH_3Li , $\text{CH}_3\text{CH}_2\text{MgBr}$, $\text{C}_6\text{H}_5\text{CH}_2\text{MgCl}$, PMe_3 , and CH_3ONa each attack $2\mathbf{t}$ from the same direction. The effective bulk of $\text{Li}(\text{C}_2\text{H}_5)_3\text{BD}$ should be considerably greater than that of an isolated D^- . Thus it seems highly unlikely that $\text{Li}(\text{C}_2\text{H}_5)_3\text{BD}$ would stereospecifically attack one benzylidene face of $2\mathbf{t}$ (see projection II, Scheme I), while R^- , Me_3P , and CH_3O^- nucleophiles stereospecifically attack the other. Furthermore, the dominant

(17) All least-squares refinements computed the agreement factors R and R_w according to $R = \Sigma ||F_o| - |F_c|| / \Sigma |F_o|$ and $R_w = [\Sigma w_i ||F_o| - |F_c||^2 / \Sigma w_i |F_o|^2]^{1/2}$, where F_o and F_c are the observed and calculated structure factors, respectively, and $w_i^{1/2} = 1/\sigma(F_o)$. The parameter minimized in all least-squares refinements was $\Sigma w_i ||F_o| - |F_c||^2$.

(18) (a) Caulton, K. G. *Coord. Chem. Rev.* **1981**, *38*, 1. (b) A reviewer has raised the possibility of PPh_3 dissociation during the $2\mathbf{k} \rightarrow 2\mathbf{t}$ isomerization. Free phosphines complex (with varying K_{eq}) to the benzylidene carbons of $2\mathbf{k}$ and $2\mathbf{t}$, as shown with PMe_3 below. Thus isomerization rates comparable to those in Table I cannot be obtained in the presence of added PPh_3 . However, when 0.5 equiv of $\text{P}(p\text{-C}_6\text{H}_4\text{CH}_3)_3$ is added to $2\mathbf{t}$ at 25 °C, no $[(\eta\text{-C}_5\text{H}_5)\text{Re}(\text{NO})(\text{P}(p\text{-C}_6\text{H}_4\text{CH}_3)_3)(=\text{CHC}_6\text{H}_5)]^+\text{PF}_6^-$ (independently synthesized analogously to $2\mathbf{t}$) forms.

Table III. Spectroscopic Data and Configurational Assignments of Diastereomeric Rhenium Complexes Formed by Nucleophilic Attack upon Benzyldienes 2t and 2k

complex and configuration (Re,C)	IR ν_{NO} (CH_2Cl_2), cm^{-1}	^1H NMR, a, b, δ		^{13}C NMR, b, c ppm	
		Re-CH	other	Re-C	other
 1-α-d,1-t (SS,RR)	1624	3.48 (d, 1 H) $J_{\text{H-}^{31}\text{P}} = 8.0 \text{ Hz}$	Ph (m, 20 H), 6.86–7.50		
 1-α-d,1-k (SR,RS)	1622	2.87 (d, 1 H), $J_{\text{H-}^{31}\text{P}} = 3.0 \text{ Hz}$	Ph (m, 20 H), 6.83–7.49		
 3t (SS,RR)	1633	3.94 (d of quartet, 1 H), $J_{\text{H-}^{31}\text{P}} = 7.3 \text{ Hz}$, $J_{\text{H-}^{31}\text{P}} = 4.4 \text{ Hz}$	CH ₃ (d, 3 H), 1.49, $J_{\text{H-}^{31}\text{P}} = 7.3 \text{ Hz}$; Ph (m, 20 H), 6.90–7.40	6.34, d, $J_{\text{C-}^{31}\text{P}} = 3.7 \text{ Hz}$	CH ₃ , 28.46; Ph 121.71, 125.54, 127.36, 128.38, d, $J_{\text{C-}^{31}\text{P}} = 9.8 \text{ Hz}$, 129.98, 133.57, d, $J = 9.8 \text{ Hz}$, 136.58, d, $J = 51.3 \text{ Hz}^d$
 3k (SR,RS)	1638	3.96 (pseudoquintet, 1 H), $J_{\text{H-}^{31}\text{P}} = 6.8 \text{ Hz}$, $J_{\text{H-}^{31}\text{P}} = 6.5 \text{ Hz}$	CH ₃ (d, 3 H), 1.91, $J_{\text{H-}^{31}\text{P}} = 6.8 \text{ Hz}$; Ph (m, 20 H), 6.70–7.40	7.68, d, $J_{\text{C-}^{31}\text{P}} = 3.7 \text{ Hz}$	CH ₃ , 32.48; Ph 122.02, 126.00, 127.36, 128.26, d, $J_{\text{C-}^{31}\text{P}} = 9.8 \text{ Hz}$, 129.95, 133.70, d, $J = 11.0 \text{ Hz}$, 136.53, d, $J = 51.3 \text{ Hz}^d$
 4t (SS,RR)	1634	3.79 (m, 1 H), $J_{\text{H-}^{31}\text{P}} = 5.1 \text{ Hz}$, $J_{\text{H-}^{31}\text{P}} = 4.9 \text{ Hz}$, $J_{\text{H-}^{31}\text{P}} = 10.5 \text{ Hz}$	CH ₃ (dd, 3 H) 0.37, $J_{\text{H-}^{31}\text{P}} = J_{\text{H-}^{31}\text{H}} =$ 7.0 Hz; CH ₃ H ₃ ' (m, 2 H), 1.72; Ph (m, 20 H), 6.40–7.40	16.90 ^e	CH ₃ , 16.90; CH ₃ , 35.40; Ph 121.59, 126.13, 127.32, 128.26, d, $J_{\text{C-}^{31}\text{P}} = 9.9 \text{ Hz}$, 129.91, 133.64, d, $J = 10.4 \text{ Hz}$, 136.21, d, $J = 51.2 \text{ Hz}$, 159.44
 4k (SR,RS)	1632	3.49 (pseudoquintet, 1 H), $J_{\text{H-}^{31}\text{P}} = 5.0 \text{ Hz}$, $J_{\text{H-}^{31}\text{P}} = 5.0 \text{ Hz}$, $J_{\text{H-}^{31}\text{P}} = 10.0 \text{ Hz}$	CH ₃ (dd, 3 H), 0.51, $J_{\text{H-}^{31}\text{P}} = J_{\text{H-}^{31}\text{H}} =$ 7.1 Hz; CH ₃ H ₃ ' (m, 2 H), 2.10, $J_{\text{H-}^{31}\text{P}} = 13.3 \text{ Hz}$; Ph (m, 20 H), 6.60–7.36	17.79, d,	CH ₃ , 17.13; CH ₃ , 39.52; Ph 122.03, 127.28, 128.17, d, $J_{\text{C-}^{31}\text{P}} = 10.9$ Hz, 129.92, 133.68, 133.78, d, $J = 10.3 \text{ Hz}$, 136.34, d, $J = 50.0 \text{ Hz}$, 159.15

1640	 5t (SS,RR)	4.47 (ddd, 1 H), $J_{1H\alpha-31P} = 4.5$ Hz, $J_{1H\alpha-1H\beta} = 13.2$ Hz, $J_{1H\alpha-1H\beta'} = 3.7$ Hz	4.78 (s, 5 H)	H_β (dd, 1 H), 2.88, $J_{1H\beta-1H\beta'} = 13.7$ Hz, $J_{1H\beta-1H\alpha} = 13.2$ Hz; $H_{\beta'}$ (dd, 1 H), 3.21, $J_{1H\beta'-1H\beta} = 13.7$ Hz, $J_{1H\beta'-1H\alpha} = 3.7$ Hz; Ph (m's, 25 H), 6.43–7.52, CH_2Cl_2 solvate, 5.28	14.91, d, $J_{13C-31P} = 4.0$ Hz	90.88	CH_2 , 48.40; Ph 121.64, 124.55, 126.27, 127.05, 127.38, 128.21, 128.48, d, $J_{13C-31P} = 10.8$ Hz, 129.99, 133.64, d, $J = 9.5$ Hz, 136.10, d, $J = 50.2$ Hz, 145.19, 158.48, CH_2Cl_2 solvate 53.39
1636	 5k (SR,RS)	3.82 (ddd, 1 H), $J_{1H\alpha-31P} = 4.6$ Hz, $J_{1H\alpha-1H\beta} = 4.7$ Hz, $J_{1H\alpha-1H\beta'} = 11.5$ Hz	4.72 (s, 5 H)	H_β (m, 2 H); $H_{\beta'}$, 3.35, $J_{H\beta'-1H\beta} = 13.5$ Hz; Ph (m's, 25 H), 6.39–7.42	16.62, d, $J_{13C-31P} = 4.3$ Hz	91.55	CH_2 , 52.26, d, $J_{13C-31P} = 2.6$ Hz; Ph 122.12, 124.29, 127.11, 127.21, 127.59, 128.29, d, $J_{13C-31P} = 8.9$ Hz, 130.03, 133.80, d, $J = 10.9$ Hz, 136.09, d, $J = 50.9$ Hz, 146.26, 158.26
1639	 6t (SR,RS)	4.47 (dd, 1 H), ^g $J_{1H-31P} = 23.4$ Hz, $J_{1H-31P} = 1.4$ Hz	5.23 (s, 5 H) ^g	PMe_3 (d, 9 H), 1.66, ^g $J_{1H-31P} = 12.6$ Hz; Ph (m's, 20 H), 6.87–7.46	–11.29, d, ^g $J_{13C-31P} = 31.8$ Hz	93.73 ^g	PMe_3 , 13.26, d, ^g $J_{13C-31P} = 56.2$ Hz; Ph 125.94, 129.58, d, $J_{13C-31P} = 9.8$ Hz, 129.82, 131.57, 134.50, d, $J = 12.2$ Hz, 137.25, d, $J = 53.7$ Hz, 149.57
1654	 6k (SS,RR)	4.03 (dd, 1 H), ^g $J_{1H-31P} = 17.4$ Hz, $J_{1H-31P} = 4.6$ Hz	5.30 (s, 5 H) ^g	PMe_3 (d, 9 H), 1.61, ^g $J_{1H-31P} = 12.4$ Hz; phenyl (m's, 20 H), 6.85–7.50	1.90, d, ^h $J_{13C-31P} = 30.8$ Hz	92.38 ^g	PMe_3 , 12.04, d, ^g $J_{13C-31P} = 55.6$ Hz; Ph 126.81, d, $J_{13C-31P} = 4.1$ Hz, 129.74, 129.84, d, $J = 10.9$ Hz, 130.86, d, $J = 6.8$ Hz, 131.81, 134.52, d, $J = 9.5$ Hz, 134.71, d, $J = 52.9$ Hz, 144.90, d, $J = 4.1$ Hz
1630	 7t (SR,RS)	5.97, d, 1 H, $J_{1H-31P} = 5.4$ Hz	4.66 (s, 5 H)	OCH_3 (s, 3 H), 2.55; Ph (m, 20 H), 6.90–7.58	65.60, d, $J_{13C-31P} = 7.2$ Hz	91.33	CH_3O , 59.62; Ph 122.50, 123.29, 127.44, 128.20, d, $J_{13C-31P} = 10.8$ Hz, 129.84, 133.94, d, $J = 10.9$ Hz, 136.84, d, $J = 51.6$ Hz, 157.63
1639	 7k (SS,RR)	5.75, d, 1 H, $J_{1H-31P} = 2.4$ Hz	4.89 (s, 5 H)	OCH_3 (s, 3 H), 2.67; phenyl (m, 20 H), 6.82–7.88	68.38, d, $J_{13C-31P} = 5.4$ Hz	91.19	CH_3O , 58.77; Ph 123.64, 124.96, 127.39, 128.02, d, $J_{13C-31P} = 10.2$ Hz, 129.72, 133.64, d, $J = 10.9$ Hz, 136.32, d, $J = 51.6$ Hz, 155.28

^a 200 MHz. ^b In $CDCl_3$ and referenced to internal $(CH_3)_4Si$ unless otherwise noted. ^c 50 MHz. ^d *ipso* C–C₆H₅ carbon (ca. 159 ppm) outside of spectrum width employed. ^e Obscured by CH_3 (16.9 ppm); spectrum in 50:50 $CDCl_3/C_6D_6$ shows one resonance of doublet. ^f Chemical shifts assigned by computer simulation of multiplet. ^g Spectrum recorded in CD_3CN . ^h Resonance obscured by CD_3CN ; value obtained in acetone- d_6 .

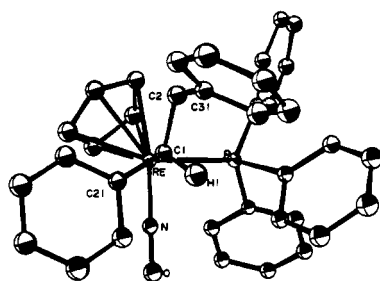
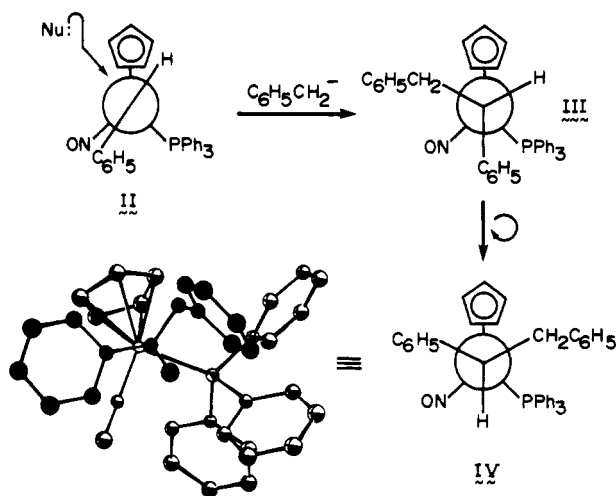


Figure 4. Stereoview of the molecular structure of $(SS,RR)-(\eta-C_5H_5)Re(NO)(PPh_3)(CH(CH_2C_6H_5)C_6H_5) \cdot CH_2Cl_2$ (**5t**· CH_2Cl_2).

Scheme II. Assignment of the Direction of Nucleophilic Attack upon **2t**



production of opposite diastereomers from **2k** requires that these nucleophiles approach I and II from the same "direction".¹⁹ Thus an X-ray structure determination of any of **3t**–**7t** or **3k**–**7k** allows configurations to be assigned to all diastereomers.

Suitable crystals of **3t** could not be grown, but single crystals of **5t** (as a CH_2Cl_2 monosolvate) were obtained by layering a CH_2Cl_2 solution with hexane. Since these crystals lost CH_2Cl_2 upon standing at room temperature, the one selected for X-ray analysis ($0.20 \times 0.25 \times 0.40$ mm) was isolated and mounted immediately prior to data collection ($-158^\circ C$, Mo $K\alpha$ irradiation as described above). The unit cell was found to be monoclinic, space group $P2_1/c$ ($Z = 4$), with lattice parameters $a = 12.027$ (4) Å, $b = 16.083$ (6) Å, $c = 18.446$ (6) Å, $\beta = 110.57$ (2)°. Of 6441 reflections with $2\theta < 50^\circ$ collected, 5309 with $I \geq 3\sigma(I)$ were used in the final refinement. Positions of all atoms, including the solvate CH_2Cl_2 , were located as outlined for **2t**· $CHCl_3$ above. The rhenium, chlorine, and phosphorus atoms were refined with anisotropic temperature factors, and all other non-hydrogen atoms were refined with isotropic thermal parameters. Hydrogen atoms were held at positions indicated from the difference Fourier map with assigned thermal parameters. The final R index was 0.025 with $R_w = 0.038$.¹⁷

The molecular structure of **5t**· CH_2Cl_2 thus obtained is shown in Figure 4. The enantiomer of the structure in Figure 4 is of course present in the unit cell as well. Absolute configurations at the chiral centers in **5t** are therefore (Re, C) S,S (Figure 4) and R,R .

The configuration of **5t** indicates that it is formed by $C_6H_5-CH_2MgCl$ attack upon the *si*-benzylidene face, antiperiplanar to the PPh_3 , as shown in Scheme II. The initially generated conformer, III, is however not the one found in the crystal. Rather, a 120° Re–C rotation occurs which orients the $-CH_2C_6H_5$ substituent between the C_5H_5 and PPh_3 ligands (IV, Scheme II). By

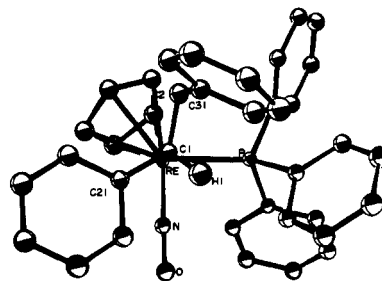


Table IV. Selected Bond Lengths and Bond Angles in **5t**· CH_2Cl_2

atoms	dist, Å	atoms	angle, deg
Re–C1	2.215 (4)	Re–C1–C2	115.7 (2)
Re–P1	2.337 (1)	Re–C1–C21	107.8 (3)
Re–N1	1.747 (3)	C1–C2–C31	114.0 (3)
Re–C ₅ H ₅ ^a	2.301	C2–C1–C21	114.7 (3)
N1–O1	1.216 (4)	N1–Re–C1	90.6 (1)
C1–C2	1.539 (5)	P1–Re–N1	90.0 (1)
C1–C21	1.502 (5)	P1–Re–C1	93.6 (1)
C2–C31	1.512 (5)	O1–N1–Re	178.3 (3)

^a Average distance from Re to C_5H_5 carbons.

assumption of an identical direction¹⁹ of attack for the other nucleophiles (vide supra), configurations are assigned to the chiral centers in **1-α-d₁-t**, **1-α-d₁-k**, **3t**–**7t**, and **3k**–**7k** as summarized in Table III.

An exhaustive list of bond distances and angles in **5t**· CH_2Cl_2 and a crystal packing diagram are provided in the supplementary material. Important bond distances and angles are summarized in Table IV. The Re–C1–C21 plane was found to make a $92.7 \pm 0.5^\circ$ angle with the least-squares plane of the Re–CHRC₆H₅ phenyl ring.

3. Stereochemistry of Hydride Abstraction from $(\eta-C_5H_5)-Re(NO)(PPh_3)(CH_2C_6H_5)$. With the absolute configurations of the enantiomers comprising **1-α-d₁-t** established, the stereochemistry of the reaction of **1-α-d₁-t** with $Ph_3C^+PF_6^-$ could be definitively probed. Proton NMR monitoring at $-70^\circ C$ (Scheme III, step b) indicated the *exclusive* formation of H^- abstraction product **2k-α-d₁** and then, upon warming (step b'), **2t-α-d₁**. Byproduct Ph_3CH was isolated. Its mass spectrum indicated Ph_3CD to be present at natural abundance level.

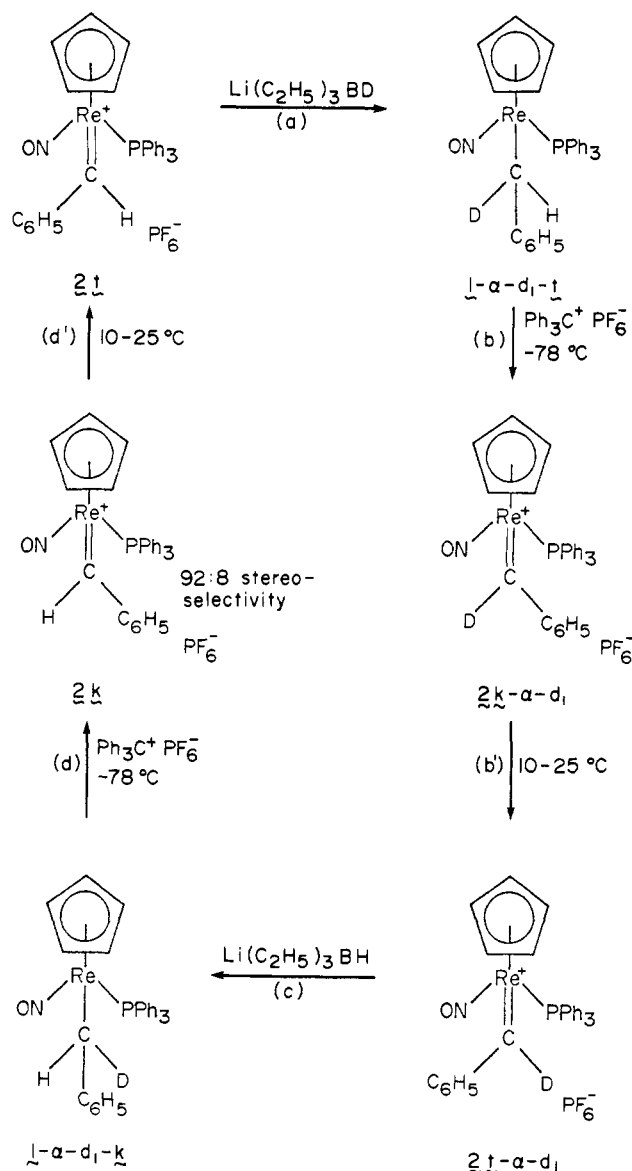
To ensure that the unusual stereospecificity of step b was not due to an extraordinary kinetic isotope effect, a closed stereochemical cycle was constructed. Thus, isolated **2t-α-d₁** was treated with $Li(C_2H_5)_3BH$ (Scheme III, step c); **1-α-d₁-k** formed stereospecifically. As little as 1% of **1-α-d₁-t** would have been detected. These results evidence a remarkable degree of metal-mediated stereocontrol over the first three steps (a, b, b', c) of the cycle.

The **1-α-d₁-k** from step c (Scheme III) was treated with $Ph_3C^+PF_6^-$ (step d). Proton NMR monitoring indicated the formation of **2k** (D^- abstraction product) and then, upon warming (step d'), **2t**. However, some Ph_3CH was evident by 1H NMR. Careful integration of $Re=CHC_6H_5$ and C_5H_5 resonances (both in situ and after isolation) indicated the product from step d' to be a $(92 \pm 2):(8 \pm 2)$ **2t-α-d₀**/**2t-α-d₁** mixture. The triphenylmethane by product was isolated; mass spectral analysis indicated a $(89 \pm 1):(11 \pm 1)$ Ph_3CD/Ph_3CH mixture.²⁰ Thus, on the order of 8–10% H^- abstraction occurs in step d.

The unusual features of Scheme III are more evident when viewed in Newman projection form (Scheme IV). In advance of any experiment, it would not have been surprising if D^- abstraction from **1-α-d₁-t** (V) had occurred (i.e., a "quasi-microscopic reverse" of D^- attack). Instead, H^- loss occurs, corresponding to

(19) We define "direction" or "side" with reference to the rhenium ligands in I and II. Nucleophilic attack upon the benzylidene carbon from a direction anti to the PPh_3 would constitute *re* face attack in I but *si* face attack in II.

(20) The Ph_3CD/Ph_3CH ratio may underestimate stereoselectivity in reactions involving predominant deuterium abstraction. For instance, we find the triphenylmethane generated by reaction of $Ph_3C^+PF_6^-$ with $(\eta-C_5H_5)-Re(NO)(PPh_3)(CD_3)$ to be a $(96 \pm 1):(4 \pm 1)$ Ph_3CD/Ph_3CH mixture. We attribute part of the Ph_3CH to side reactions involving nondeuterated ligands and/or adventitious H^- sources.

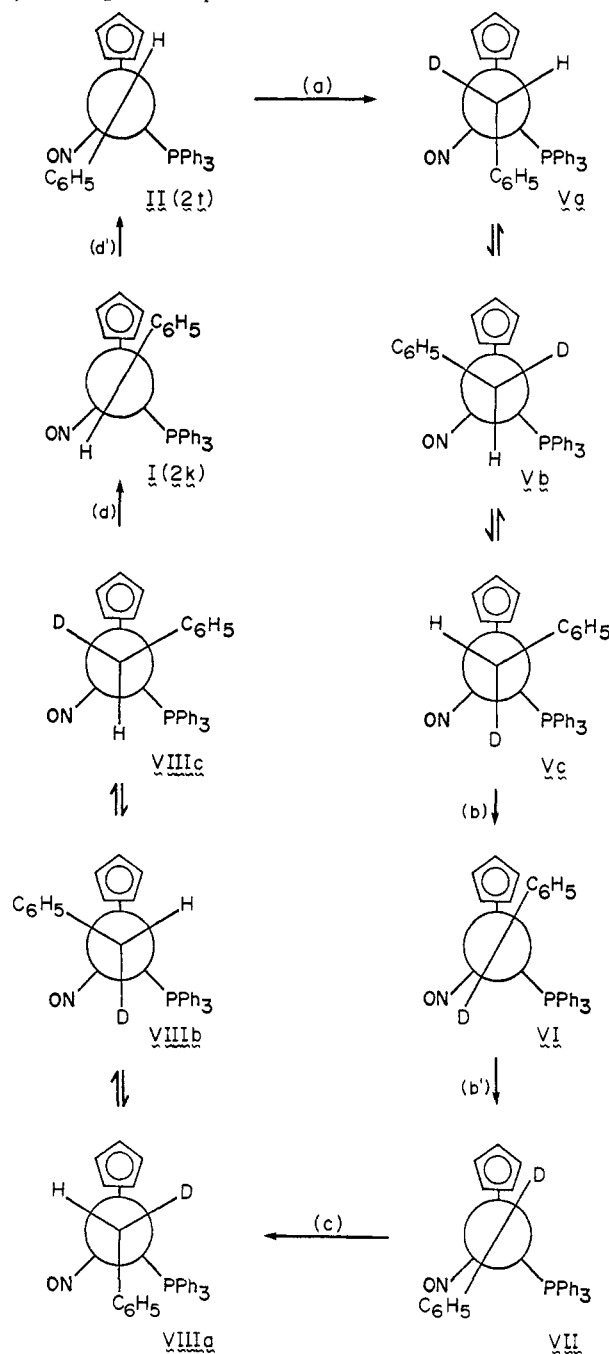
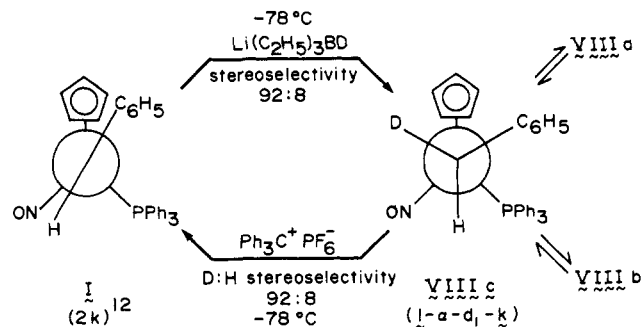
Scheme III. An Organometallic Walden-Type Cycle ("Long" Cycle)

abstraction of the *pro-R* α -hydride from $(\eta\text{-C}_5\text{H}_5)\text{Re}(\text{NO})(\text{PPh}_3)(\text{CH}_2\text{C}_6\text{H}_5)$ (**1**). Possible rationales for this reactivity will be presented in the Discussion.

A "short" cycle, interconverting **2k** and **1- α -d₁-k** as shown in Scheme V, is implicit in the reactions described above. The simplicity of Scheme V vis-à-vis the complexity of Scheme IV can be explained as follows, without reference to mechanism. When the cycle is started with **2k** (Scheme V), D^- is delivered into what would be the *pro-R* position of **1**. Hence D^- is abstracted in the subsequent step with $\text{Ph}_3\text{C}^+\text{PF}_6^-$. However, when the cycle is started with **2t** (Scheme IV), D^- is delivered into what would be the *pro-S* position of **1**. Hence H^- is abstracted in the subsequent step with $\text{Ph}_3\text{C}^+\text{PF}_6^-$.

4. Additional Experiments Related to Reaction Stereocontrol.

Further experiments were conducted to provide insight into Schemes I-V. First, the α -proton $J_{\text{H-P}}(\text{H})$ in the ^1H NMR spectrum of **1** in CDCl_3 were examined as a function of temperature. The data shown in Table V were obtained. Couplings measured in CD_2Cl_2 were similar. As will be described in the Discussion, $J_{\text{H-P}}(\text{H})$ values have been previously correlated to conformer populations (e.g., Va-c) in $(\eta\text{-C}_5\text{H}_5)\text{Fe}(\text{CO})(\text{PX}_3)(\text{CH}_2\text{R})$ systems.²¹

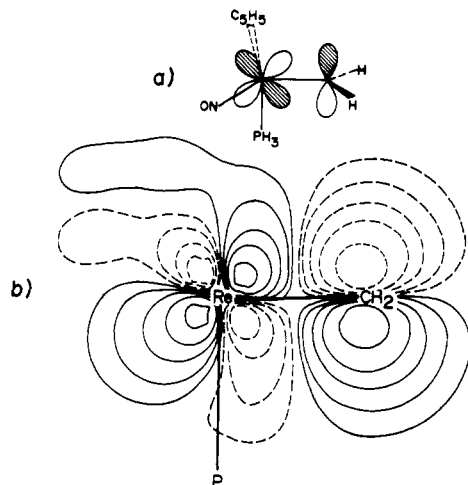
Scheme IV. Newman Projections of Species Involved in Scheme III, Including All $1\text{-}\alpha\text{-d}_1$ Rotamers**Scheme V.** A "Short" Cycle

Second, the dissymmetry of the Hückel orbitals with respect to the $\text{Re}=\text{CHR}$ plane (which could provide an *electronic* basis for the nonequivalent reactivities of the two diastereotopic al-

Table V. Variation of ^{31}P - ^1H and ^1H - ^1H NMR Coupling Constants (Hz)^b in $(\eta\text{-C}_5\text{H}_5)\text{Re}(\text{NO})(\text{PPh}_3)(\text{CH}_2\text{C}_6\text{H}_5)$ with Temperature^a

temp, K	$J_{^{31}\text{P}-^1\text{H}_\alpha}$	$J_{^{31}\text{P}-^1\text{H}_\alpha'}$	$J_{^1\text{H}_\alpha-^1\text{H}_\alpha'}$
320	7.64	3.16	11.70
310	7.74	3.10	11.70
300	7.86	3.04	11.72
290	7.88	2.92	11.72
280	7.81	2.83	11.73
270	7.92	2.75	11.72
260	7.90	2.60	11.75
250	7.82	2.32	11.70
240	7.78	2.26	11.72

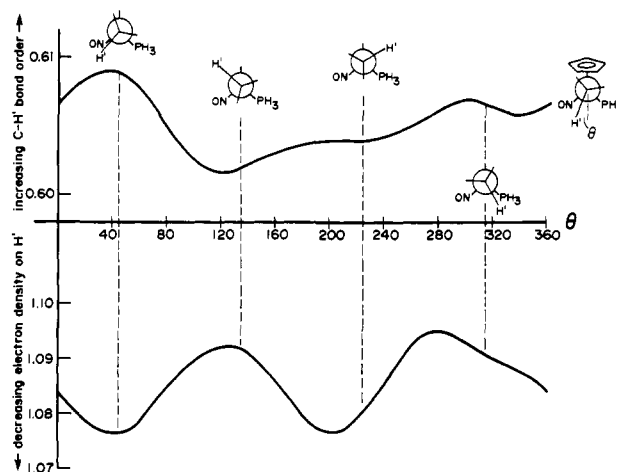
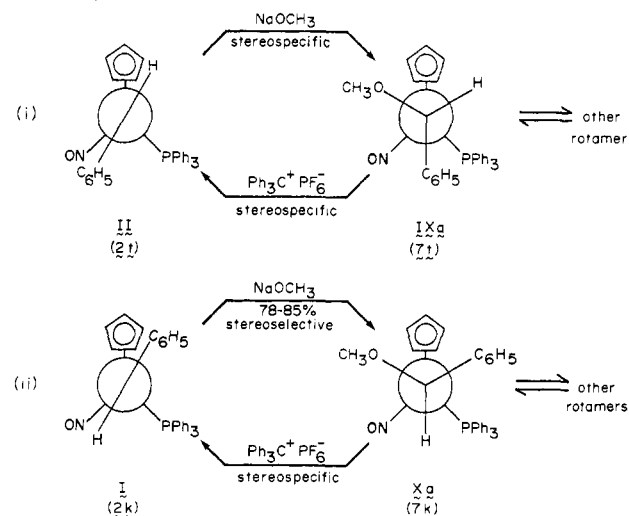
^a In CDCl_3 ; data are the average of two runs. ^b Spectra were recorded at 0.061 Hz/data point. Low-temperature coupling constants are less accurate than the others due to peak broadening.

**Figure 5.** LUMO of $[(\eta\text{-C}_5\text{H}_5)\text{Re}(\text{NO})(\text{PPh}_3)(=\text{CH}_2)]^+$: (a) schematic; (b) contour diagram (for $\Psi = \pm 0.20, \pm 0.15, \pm 0.10, \pm 0.05, \pm 0.01$) in P-Re-C plane.

kylidene faces) was examined. In the model compound $[(\eta\text{-C}_5\text{H}_5)\text{Re}(\text{NO})(\text{PPh}_3)(=\text{CH}_2)]^+$, the LUMO was found to be the $d\text{-p}$ π antibonding combination. This orbital should command the major interaction with the incoming nucleophile, but as shown in Figure 5, it is *symmetrical* with respect to the $\text{Re}=\text{CH}_2$ plane. A model nucleophile, H^- , was placed 2 Å from the methyldiene in $[(\eta\text{-C}_5\text{H}_5)\text{Re}(\text{NO})(\text{PPh}_3)(=\text{CH}_2)]^+$. The total energy indicated a slight preference for an approach antiperiplanar (over synperiplanar) to the PPh_3 .

Third, properties of the model alkyl $(\eta\text{-C}_5\text{H}_5)\text{Re}(\text{NO})(\text{PPh}_3)(\text{CH}_3)$ were also probed via extended Hückel MO calculations. The barrier to rotation about the $\text{Re}-\text{CH}_3$ bond was found to be ~ 3 kcal/mol, with a staggered conformation (hydrogen antiperiplanar to C_5H_5) as energy minimum. As the $\text{Re}-\text{CH}_3$ bond was rotated, no particular weakening (bond-order decrease) of any $\text{C}-\text{H}$ bond was noted. One $\text{C}-\text{H}$ bond of the $\text{Re}-\text{CH}_3$ group ($\text{C}-\text{H}'$) was elongated from 1.09 to 1.40 Å in order to more closely resemble a hydride abstraction transition state. Now as the $\text{Re}-\text{CH}_2\text{H}'$ bond was rotated, a significant weakening of the $\text{C}-\text{H}'$ bond (and increase of electron density on H') occurred when it was antiperiplanar to the PPh_3 ligand (see Figure 6).

Finally, reactions of **7t** and **7k** with $\text{Ph}_3\text{C}^+\text{PF}_6^-$ were also investigated.⁸ When **7t** was treated with $\text{Ph}_3\text{C}^+\text{PF}_6^-$ at -78°C in a ^1H NMR monitored reaction, **2t** was observed to form exclusively. Thus CH_3O^- is chemospecifically²² and stereospecifically abstracted. Coupled with the reaction of **2t** and NaOCH_3 described above, this reaction completes a second "short cycle", as shown in Scheme VI. Similarly, when a 90:10 **7k/7t** mixture was treated with $\text{Ph}_3\text{C}^+\text{PF}_6^-$ at -78°C , a 90:10 **2k/2t** mixture

**Figure 6.** Calculated change in $\text{C}-\text{H}'$ bond order and electron density on H' as the $\text{Re}-\text{C}$ σ bond in $(\eta\text{-C}_5\text{H}_5)\text{Re}(\text{NO})(\text{PPh}_3)(\text{CH}_2\text{H}')$ is rotated through 360° ($\text{C}-\text{H}' =$ bond arbitrarily elongated to 1.4 Å).**Scheme VI.** "Short" Cycles Involving CH_3O^- Addition/Abstraction

formed. Thus CH_3O^- is stereospecifically abstracted from **7k**, closing the other short cycle in Scheme VI. These data require that $^-\text{OCH}_3$ attack and $^-\text{OCH}_3$ abstraction occur from the same "side"¹⁹ of the complex.

Discussion

1. Benzylidene Complexes: Structure and Bonding. To our knowledge, the existence of geometric isomers due to metal-carbon multiple bonding is without precedent. Commonly used terms for distinguishing geometric isomers (*cis/trans*; *Z/E*) are clearly inadequate for **2k** and **2t**. According to IUPAC nomenclature,²³ **I (2k)** and **II (2t)** are unambiguously designated as *synclinal (sc)* and *anticlinal (ac)*, respectively.

Absolute configurations at rhenium are assigned according to the Baird-Sloan modification of the Cahn-Ingold-Prelog priority rules.²⁴ The C_5H_5 ligand is considered to be a pseudoatom of atomic number 30. Hence all figures in this paper have have an *S*-rhenium configuration.

As has been observed with other metals and unsaturated ligands,¹⁴ extended Hückel calculations accurately predict rhenium alkylidene bonding geometries. The optimal alkylidene position

(23) *Pure Appl. Chem.* **1976**, *48*, 11. See section E-5.6, p 24. A *synclinal* conformer of **2** is one in which the highest priority²⁴ groups on $\text{Re}(\text{C}_5\text{H}_5)$ and $\text{C}(\text{C}_6\text{H}_5)$ define a $60 \pm 30^\circ$ torsion angle. An *anticlinal* conformer is one in which the highest priority groups define a $120 \pm 30^\circ$ torsion angle.

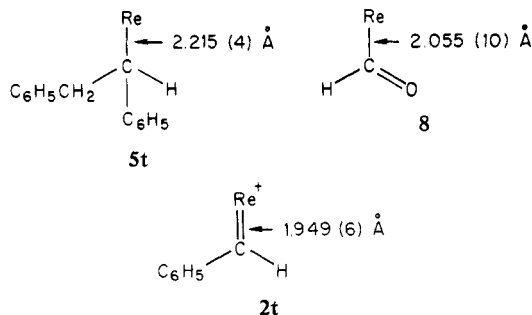
(24) (a) Stanley, K.; Baird, M. C. *J. Am. Chem. Soc.* **1975**, *97*, 6598. (b) Sloan, T. *Top. Stereochem.* **1981**, *12*, 1.

(22) Trost, B. M.; Salzmann, T. N. *J. Am. Chem. Soc.* **1973**, *95*, 6840. See footnote 12.

is obtained when the empty p orbital of the carbene fragment (counted as neutral) maximally overlaps the highest occupied d orbital of the metal fragment. In a d^6 metal fragment such as $(\eta\text{-C}_5\text{H}_5)\text{Mn}(\text{CO})_2$, which has a plane of symmetry, the highest occupied d orbital would be in a horizontal plane in the Newman projections perspectives utilized in this paper.¹⁴ Accordingly, the X-ray crystal structure of $(\eta\text{-C}_5\text{H}_5)\text{Mn}(\text{CO})_2(=\text{C}(\text{CH}_3)_2)$ ($\text{Mn}=\text{C}$ distance = 1.868 Å) shows that the alkylidene plane bisects the C_5H_5 ring.²⁵ In $(\eta\text{-C}_5\text{H}_5)\text{Re}(\text{NO})(\text{PPh}_3)^+$ (and related isoelectronic metal fragments), no symmetry is maintained and the highest occupied d orbital rotates into a plane containing the Re-P bond (compare to Figure 5),¹⁴ resulting in alkylidene geometries I and II.

The crystal structures of three benzylidene complexes, $(\eta\text{-C}_5\text{H}_5)_2\text{Ta}(\text{CH}_2\text{C}_6\text{H}_5)(=\text{CHC}_6\text{H}_5)$,²⁶ $(\eta\text{-C}_5\text{Me}_5)\text{Ta}(\text{CH}_2\text{C}_6\text{H}_5)_2(=\text{CHC}_6\text{H}_5)$,²⁷ and $(\eta\text{-C}_5\text{H}_5)_2\text{W}=\text{CHC}_6\text{H}_5$,²⁸ have been previously reported. Since these all contain third-row metals, their bonding features may be closely compared to **2t**. For the first and third complexes, $\text{M}=\text{C}_{\text{ipso}}$ bond angles are reasonably close to those expected for sp^2 carbons (135° , 133°), and $\text{M}=\text{C}_{\alpha}$ bond lengths are 2.07 and 2.05 Å, respectively. However, $(\eta\text{-C}_5\text{Me}_5)\text{Ta}(\text{CH}_2\text{C}_6\text{H}_5)_2(=\text{CHC}_6\text{H}_5)$ is a 14-electron complex, so the benzylidene ligand adopts a "T" shaped²⁹ geometry ($\angle\text{Ta}=\text{C}_{\alpha}-\text{C}_{\text{ipso}} = 160^\circ$, with a proposed $\angle\text{Ta}=\text{C}_{\alpha}-\text{H}$ of ca. 90°) to help relieve the electron deficiency. A short $\text{Ta}=\text{C}_{\alpha}$ distance of 1.88 Å was also noted. Benzylidene **2t** is an 18-electron complex, and accordingly its $\angle\text{Re}=\text{C}_{\alpha}-\text{C}_{\text{ipso}}$ of 136° more closely resembles the former class of complexes. The $^+\text{Re}=\text{C}_{\alpha}$ distance in **2t**, 1.949 (6) Å, is intermediate between the two types of complexes. The bond contraction vis-à-vis $(\eta\text{-C}_5\text{H}_5)_2\text{W}=\text{CHC}_6\text{H}_5$ may be due to the positive charge on rhenium.

Together with the X-ray structure of the formyl $(\eta\text{-C}_5\text{H}_5)\text{Re}(\text{NO})(\text{PPh}_3)(\text{CHO})$ (**8**),³⁰ this study marks the first time that accurate metal-carbon bond lengths have been determined for a homologous series of alkyl, formyl, and alkylidene complexes.³¹ As shown below, the $\text{Re}-\text{C}_{\alpha}$ distances decrease as the π -acceptor capabilities of the ligands increase. The $\text{Re}-\text{C}_{\alpha}$ distance in formyl **8** is closer to that of benzylidene **2t** than it is to alkyl **5t**. This supports our previous conclusion^{15b,30} that a dipolar alkylidene-like resonance form $^+\text{Re}=\text{C}(\text{H})\text{O}^-$ makes a substantial contribution to the ground state of **8**.



The activation parameters for **2k** \rightarrow **2t** isomerization contain a component arising from steric interactions. In view of recent data on homologous vinylidene complexes $[(\eta\text{-C}_5\text{H}_5)\text{Re}(\text{NO})-$

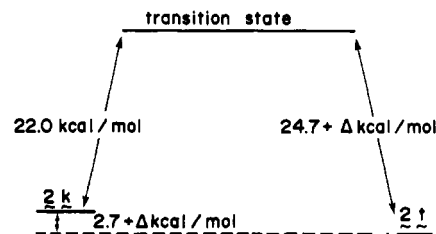


Figure 7. ΔG and ΔG^\ddagger for the interconversion of **2k** and **2t** at 25 °C.

$(\text{PPh}_3)(=\text{C}=\text{CRR}')^+]$, where steric effects should be attenuated,³² we estimate the d-p π bond strength in **2** to be on the order of 15 ± 2 kcal/mol. A $\text{Re}=\text{CH}_2$ rotational barrier (which also should involve minimal steric interactions) has not yet been obtained for $[(\eta\text{-C}_5\text{H}_5)\text{Re}(\text{NO})(\text{PPh}_3)(=\text{CH}_2)]^+\text{PF}_6^-$, but the fact that no coalescence of the $=\text{CH}_2$ ^1H NMR resonances occurs at 27 °C bounds ΔG^\ddagger_{27} as >15 kcal/mol.^{15b}

Rotational barriers of other electrophilic alkylidene complexes have proven to be much lower.³³ For instance, ΔG^\ddagger for $=\text{CH}_2$ rotation in $[(\eta\text{-C}_5\text{H}_5)\text{Fe}(\text{PPh}_2\text{CH}_2\text{CH}_2\text{PPh}_2)(=\text{CH}_2)]^+\text{CF}_3\text{SO}_3^-$ is only (despite strong donor ligands and the absence of good π -acceptor ligands on iron) 10.4 ± 0.1 kcal/mol over the temperature range of -65 to -14 °C.^{33a} This probably reflects intrinsic differences in first-row vs. third-row metal-ligand π -bond strengths. Rotational barriers of two unstable $\text{W}=\text{CH}_2$ complexes, $[(\eta\text{-C}_5\text{H}_5)\text{W}(\text{CO})_2(\text{PPh}_3)(=\text{CH}_2)]^+\text{AsF}_6^-$ and $[(\eta\text{-C}_5\text{H}_5)\text{W}(\text{CO})_2(\text{PET}_3)(=\text{CH}_2)]^+\text{AsF}_6^-$, have been determined to be 8.3 ± 0.1 and 9.0 ± 0.1 kcal/mol, respectively.^{33b} These low values may result from the presence of two good π -accepting CO ligands on each tungsten. Schrock has measured the $\text{Ta}=\text{CH}-\text{C}_6\text{H}_5$ rotational barrier (which interconverts enantiomers) of the nucleophilic benzylidene complex $(\eta\text{-C}_5\text{H}_5)_2\text{Ta}(\text{CH}_2\text{C}_6\text{H}_5)(=\text{CHC}_6\text{H}_5)$.²⁶ A ΔG^\ddagger of 19.2 ± 0.2 kcal/mol, comparable to that observed for other tantalum alkylidene complexes,²⁶ was determined.

Alkylidene complexes of the formula $[(\eta\text{-C}_5\text{H}_5)\text{Fe}(\text{CO})(\text{PPh}_3)(=\text{CHR})]^+$, which are expected¹⁴ to be isostructural with **2** and its aliphatic homologues, have been extensively studied by Brookhart.^{11,34} The fact that these have not been observed to exist in two geometric isomeric forms (despite in some cases having been generated from diastereomeric $(\eta\text{-C}_5\text{H}_5)\text{Fe}(\text{CO})(\text{PPh}_3)(\text{CH}(\text{OCH}_3)\text{R})$ complexes at -78 °C) is understandable in view of the above rotational barrier data.

Although ^1H NMR indicates that $\leq 1\%$ of **2k** is in equilibrium with **2t** at 25 °C, we do not believe that K_{eq} is significantly greater than 99.³⁵ For instance, aliphatic homologues of **2**, such as propylidene $[(\eta\text{-C}_5\text{H}_5)\text{Re}(\text{NO})(\text{PPh}_3)(=\text{CHCH}_2\text{CH}_3)]^+\text{PF}_6^-$, exist as $(91 \pm 2):(9 \pm 2)$ equilibrium mixtures of anticlinal and synclinal isomers. If the **2t/2k** K_{eq} is assumed to be slightly greater than 99, then $\Delta G_{25} = -2.7 - \Delta$ kcal/mol, where Δ is a small increment. From ΔH^\ddagger (20.9 ± 0.4 kcal/mol) and ΔS^\ddagger (-3.8 ± 0.2 eu), a ΔG^\ddagger_{25} of 22.0 kcal/mol can be calculated. This enables the construction of the energy diagram shown in Figure 7.

The 365-nm absorption in the UV-visible spectrum of **2t** (Figure 3) is possibly a $n \rightarrow \pi^*$ transition involving a LUMO of the type in Figure 5.¹⁴ It is absent in aliphatic homologues such as the cream-colored propylidene $[(\eta\text{-C}_5\text{H}_5)\text{Re}(\text{NO})(\text{PPh}_3)(=\text{CHCH}_2\text{CH}_3)]^+\text{PF}_6^-$.⁹ These undergo analogous photoisomerization but exhibit only an extended tail into the visible region. The mechanism of the photoisomerization **2t** \rightarrow **2k** is presently under study.⁹ In view of the wealth of metal alkylidene ground-state chemistry, many intriguing possibilities exist for metal

(25) Friedrich, P.; Besl, G.; Fischer, E. O.; Huttner, G. *J. Organomet. Chem.* **1977**, *139*, C68.

(26) Schrock, R. R.; Messerle, L. W.; Wood, C. D.; Guggenberger, L. J. *J. Am. Chem. Soc.* **1978**, *100*, 3793.

(27) Messerle, L. W.; Jennische, P.; Schrock, R. R.; Stucky, G. *J. Am. Chem. Soc.* **1980**, *102*, 6744.

(28) Marsella, J. A.; Folting, K.; Huffman, J. C.; Caulton, K. G. *J. Am. Chem. Soc.* **1981**, *103*, 5596.

(29) Goddard, R. J.; Hoffmann, R.; Jemmis, E. D. *J. Am. Chem. Soc.* **1980**, *102*, 7667.

(30) Wong, W.-K.; Tam, W.; Strouse, C. E.; Gladysz, J. A. *J. Chem. Soc., Chem. Commun.* **1979**, 530.

(31) (a) An X-ray crystal structure of optically pure $(-)\text{-R}-(\eta\text{-C}_5\text{H}_5)\text{Re}(\text{NO})(\text{PPh}_3)(\text{CH}_2\text{C}_6\text{H}_5)$ has also been completed and will be described in a separate publication.^{31b} The $\text{Re}-\text{C}_{\alpha}$ bond distance was found to be 2.203 (8) Å. (b) Merrifield, J. H.; Strouse, C. E.; Gladysz, J. A. *Organometallics*, in press.

(32) Wong, A.; Gladysz, J. A. *J. Am. Chem. Soc.* **1982**, *104*, 4948.

(33) (a) Brookhart, M.; Tucker, J. R.; Flood, T. C.; Jensen, J. *J. Am. Chem. Soc.* **1980**, *102*, 1203. (b) Kegley, S. E.; Brookhart, M.; Husk, G. R. *Organometallics* **1982**, *1*, 760.

(34) Brookhart, M.; Tucker, J. R.; Husk, G. R. *J. Am. Chem. Soc.* **1981**, *103*, 979.

(35) When crystals of optically pure **2t** are dissolved, a slight mutarotation occurs. This sensitive criterion suggests the presence of small equilibrium concentrations of **2k**.^{31b}

alkylidene excited-state chemistry.

2. Benzylidenes 2t and 2k: Stereochemistry of Nucleophilic Attack. While the LUMO of the model system $[(\eta\text{-C}_5\text{H}_5)\text{Re}(\text{NO})(\text{PH}_3)(=\text{CH}_2)]^+$ reveals no distortion with respect to the $\text{Re}=\text{C}$ plane (Figure 5), such dissymmetries are usually minute. Dissymmetries in the π system of organic alkenes and carbonyl compounds (measured by the mixing of s and p coefficients) are usually on the order of magnitude of 10^{-3} (ratio of s to p) but nonetheless predict the stereochemical course of addition reactions.³⁶ While our findings do not exclude electronic effects from contributing to the stereospecific attack of nucleophiles upon **2t** (for instance, the participation of low-lying antiperiplanar σ^* orbitals in nucleophilic attack upon organic π systems is well documented,³⁷ and we did calculate an energetic preference for H^- approach antiperiplanar to the $\text{Re}-\text{PH}_3$ bond), more elaborate calculations are required to probe this point.

In view of the above, we ascribe the stereospecificity of nucleophilic attack upon **2t** primarily to steric effects. As can easily be seen in Figure 2, the *re* face of the benzylidene ligand is shielded by the bulky PPh_3 ligand. Thus nucleophilic attack occurs on the *si* face, as indicated by the molecular structure of **5t** (Figure 2 and Scheme II). The ca. 90° angle of the $\text{Re}-\text{C}1-\text{C}21$ plane in **5t** with the adjacent phenyl ring suggests a hyperconjugative interaction. This may be a factor in the crystallization of **5t** in rotamer IV.

It is not uncommon for the less stable of two isomers to exhibit slightly lower reaction stereoselectivity. Hence the 92–95% stereoselectivity generally observed in nucleophilic attack upon **2k** is understandable. As noted previously, nucleophilic attack upon **2t** and **2k** occurs preferentially from the same direction.¹⁹

There are at least two important general factors that can influence the stereochemistry of alkylidene attack: (a) the alkyl group in $\text{Re}=\text{CHR}$; (b) the size of the phosphine. Experimental details of these studies will be reported separately, but two key results will be summarized here.³⁸

First, the ethylidene complex $[(\eta\text{-C}_5\text{H}_5)\text{Re}(\text{NO})(\text{PPh}_3)(=\text{CHCH}_3)]^+\text{PF}_6^-$ exists as a $(90 \pm 2):(10 \pm 2)$ equilibrium mixture of anticlinal²³ (e.g., II) and synclinal (e.g., I) geometric isomers. Upon reaction with $\text{Li}(\text{C}_2\text{H}_5)_3\text{BD}$, a $(89 \pm 2):(11 \pm 2)$ mixture of diastereomers of $(\eta\text{-C}_5\text{H}_5)\text{Re}(\text{NO})(\text{PPh}_3)(\text{CHDCH}_3)$ is produced. We therefore conclude that the size of the $\text{Re}=\text{CHR}$ alkyl group does not significantly influence the direction of nucleophilic attack.

Second, the PMe_3 complex $(\eta\text{-C}_5\text{H}_5)\text{Re}(\text{NO})(\text{PMe}_3)(\text{CH}_2\text{C}_6\text{H}_5)$ has been prepared. When $(\eta\text{-C}_5\text{H}_5)\text{Re}(\text{NO})(\text{PMe}_3)(\text{CH}_2\text{C}_6\text{H}_5)$ is treated with $\text{Ph}_3\text{C}^+\text{PF}_6^-$ in CD_2Cl_2 at -78°C , a single geometric isomer of $[(\eta\text{-C}_5\text{H}_5)\text{Re}(\text{NO})(\text{PMe}_3)(=\text{CHC}_6\text{H}_5)]^+\text{PF}_6^-$ forms. No isomerization is observed upon warming to room temperature or heating to 60°C in CDCl_3 . Subsequent reaction of $[(\eta\text{-C}_5\text{H}_5)\text{Re}(\text{NO})(\text{PMe}_3)(=\text{CHC}_6\text{H}_5)]^+\text{PF}_6^-$ with $\text{Li}(\text{C}_2\text{H}_5)_3\text{BD}$ at -78°C yields $(\eta\text{-C}_5\text{H}_5)\text{Re}(\text{NO})(\text{PMe}_3)(\text{CHDC}_6\text{H}_5)$ as a $(77 \pm 1):(23 \pm 1)$ mixture of diastereomers. Thus a bulky phosphine is necessary for high stereoselectivity.

3. Stereochemistry of the Reactions of Rhenium Alkyls with $\text{Ph}_3\text{C}^+\text{PF}_6^-$. The data in Schemes III–V show that $\text{Ph}_3\text{C}^+\text{PF}_6^-$ preferentially abstracts the hydride or deuteride corresponding to the *pro-R* α hydrogen of **1**. A deuterium isotope effect would be expected to enhance the stereoselectivity of step b ($>99:1$) in Schemes III and IV while diminishing the stereoselectivity of step d ($(92 \pm 2):(8 \pm 2)$). If a $k_{\text{H}}/k_{\text{D}}$ in the 4–7 range is assumed,

the intrinsic stereoselectivity for *pro-R* α -hydride abstraction from **1** is on the order of 99–98:1–2. We now consider the mechanistic implications of this selectivity.

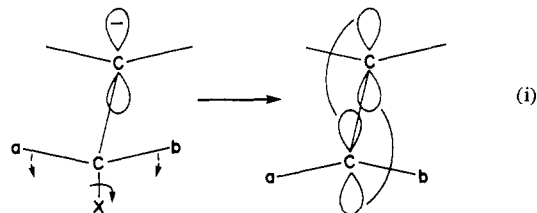
An important question is whether the $\text{Re}-\text{C}$ rotamers of **1** (or Va–c, VIIa–c, Scheme IV) are rapidly interconverting on the time scale of the reaction of **1** with $\text{Ph}_3\text{C}^+\text{PF}_6^-$. A variety of methods have been used to probe rotational barriers about transition-metal–carbon σ bonds.^{21,39} Values in the 3–6 kcal/mol range have generally been obtained for $\text{L}_n\text{M}-\text{CH}_3$ complexes, in reasonable agreement with that calculated above for $(\eta\text{-C}_5\text{H}_5)\text{Re}(\text{NO})(\text{PH}_3)(\text{CH}_3)$. More congested transition-metal alkyls (such as $(\eta\text{-C}_5\text{H}_5)\text{Fe}(\text{CO})_2[\text{C}(\text{SCH}_3)_3]$, $\Delta G^\ddagger \approx 8.7$ kcal/mol)^{39b} have rotational barriers approaching 10 kcal/mol. However, there is no evidence for any coalescence phenomena in the 200-MHz ^1H NMR spectrum of **1** as the temperature is varied from 50 to -85°C .

Baird has addressed the question of metal–carbon σ -bond rotation in $(\eta\text{-C}_5\text{H}_5)\text{Fe}(\text{CO})(\text{PPh}_3)(\text{CH}_2\text{C}_6\text{H}_5)$,²¹ which is isostructural with **1**. If the α -hydrogen $J_{\text{31P}-^1\text{H}}$ values exhibit a Karplus-like geometry dependence, then a change in temperature will, in the case of equilibrating rotamers, alter the relative rotamer populations and hence the observed $J_{\text{31P}-^1\text{H}}$. Baird in fact noted that the $J_{\text{31P}-^1\text{H}}$ varied smoothly with temperature. Our similar experiment with **1** (Table V) shows that one $J_{\text{31P}-^1\text{H}}$ shifts smoothly with temperature, while the other fluctuates over the narrow range of 7.64–7.92 Hz. The geminal coupling constants, $J_{\text{H}_a-\text{H}_b}$, which should change only minutely with temperature, are included (Table V) to provide an idea of the intrinsic scatter in the data. Thus it is clear that rotamers of **1** interconvert over the temperature range examined.

From the assumption that $J_{\text{31P}-^1\text{H}_a} = 17 \pm 1$ Hz when the phosphorus is antiperiplanar to hydrogen and 0 ± 1 Hz when the phosphorus is gauche to hydrogen, Baird concluded (by extrapolating his data to absolute zero) that the rotamer of $(\eta\text{-C}_5\text{H}_5)\text{Fe}(\text{CO})(\text{PPh}_3)(\text{CH}_2\text{C}_6\text{H}_5)$ corresponding to Va/VIIa (Scheme IV) is the thermodynamically most stable. A similar analysis of our data with **1** (Table V) suggests that Va and Vb (or VIIa and VIIb) type rotamers are of approximately equal energies. In crystalline **1**, only a Vb (or VIIb) type rotamer is present.^{31b} The most important conclusion, for our purposes, from this and Baird's study—and one that we think is reasonable on intuitive grounds alone—is that Vc (or VIIc) type rotamers are the *least* stable. These force a phenyl ring to reside between the bulky PPh_3 and C_5H_5 ligands.

Hence, in the absence of evidence to the contrary, we assume that rotamers of **1** rapidly interconvert at -78°C and that any are available for reaction with $\text{Ph}_3\text{C}^+\text{PF}_6^-$. We now consider two classes of mechanisms for the reactions of rhenium alkyls with $\text{Ph}_3\text{C}^+\text{PF}_6^-$: (a) “conventional” mechanisms which have analogy in C=C double-bond-forming reactions, and (b) “new” mechanisms which are without established precedent.

We visualize the abstraction of an X^- group from $(\eta\text{-C}_5\text{H}_5)\text{Re}(\text{NO})(\text{PPh}_3)(\text{CHXR})$ by $\text{Ph}_3\text{C}^+\text{PF}_6^-$ as being closely related to the second step of an E1cB elimination reaction (eq i).⁴⁰ As



(36) (a) Klein, J. *Tetrahedron Lett.* **1973**, 4307; *Tetrahedron* **1974**, 30, 3349. (b) Nguyen, Trong Anh; Eisenstein, O.; Lefour, J. M.; Tran Huu Dau, M. E. *J. Am. Chem. Soc.* **1973**, 95, 6146. (c) Liotta, C. L. *Tetrahedron Lett.* **1975**, 519. (d) Liotta, C. L.; Burgess, E. M. *J. Org. Chem.* **1981**, 46, 1703. (e) Inagaki, S.; Fukui, K. *Chem. Lett.* **1974**, 509. (f) Inagaki, S.; Fujimoto, H.; Fukui, K. *J. Am. Chem. Soc.* **1976**, 98, 4054. (g) Eisenstein, O.; Klein, J.; Lefour, J. M. *Tetrahedron* **1979**, 35, 225.

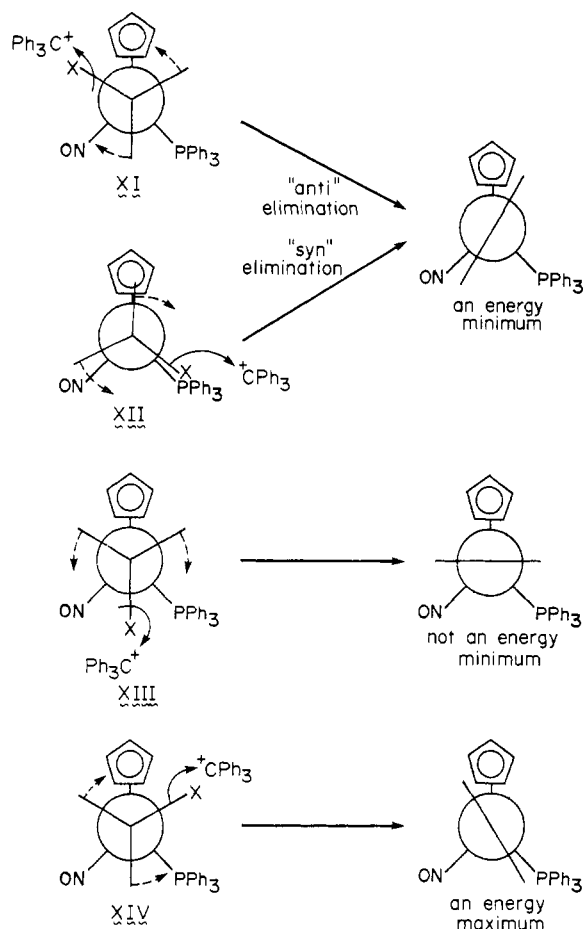
(37) (a) Nguyen, Trong Anh; Eisenstein, O. *Nouv. J. Chim.* **1977**, 1, 61. (b) Huet, J.; Maroni-Barnaud, Y.; Nguyen, Trong Anh; Seyden-Penne, J. *Tetrahedron Lett.* **1976**, 159. (c) Caramella, P.; Rondan, N. G.; Paddon-Row, M. N.; Houk, K. N. *J. Am. Chem. Soc.* **1981**, 103, 2438.

(38) Kiel, W. A. Ph.D. Thesis, UCLA, 1982.

(39) (a) Jordan, R. F.; Tsang, E.; Norton, J. R. *J. Organomet. Chem.* **1978**, 149, C53 and references therein. (b) McCormick, F. B.; Angelici, R. J.; Pickering, R. A.; Wagner, R. E.; Jacobson, R. A. *Inorg. Chem.* **1981**, 20, 4108.

(40) (a) Lowry, T. H.; Richardson, K. S. “Mechanism and Theory in Organic Chemistry”, 2nd ed.; Harper and Row: New York, 1981; pp 530–556 and references therein. (b) For related lone-pair effects in organic reactions, see: Deslongchamps, P. *Tetrahedron* **1975**, 31, 2463. Wolfe, S. *Acc. Chem. Res.* **1972**, 5, 102.

Scheme VII. Possible "Elimination-Type" Transition States for Abstraction of X^- from $(\eta\text{-C}_5\text{H}_5)\text{Re}(\text{NO})(\text{PPh}_3)(\text{CHXR})$ by $\text{Ph}_3\text{C}^+\text{PF}_6^-$



shown, a lone pair assists in the departure of leaving group X^- ; X^- departs in a periplanar fashion such that as the carbon is rehybridized from sp^3 to sp^2 , substituents a and b move toward their new energy minima. Other transition-state structures are of much higher energy.⁴⁰

As previously noted, $(\eta\text{-C}_5\text{H}_5)\text{Re}(\text{NO})(\text{PPh}_3)(\text{CHXR})$ alkyls have a high-lying d orbital "lone pair" on rhenium. Thus in Scheme VII, we consider transition states that are related to eq i. In the first two, XI and XII, the rhenium fragment lone pair is positioned to anchimerically assist the departure of X^- , and the concomitant rehybridization of the alkyl carbon leads directly to the product ground-state geometry. Both of these features are absent in transition states XIII and XIV (and their eclipsed variants), and hence they are rejected.

Transition state XI is an "anti" elimination with respect to PPh_3 , whereas XII is a "syn" elimination. These can be distinguished on stereochemical grounds. Consider the "short" CH_3O^- addition/elimination cycles in Scheme VI. It can be readily seen that only the "anti" transition state converts IXa (**7t**) to II (**2t**), and Xa (**7k**) to I (**2k**). The "syn" transition state (XII) would give alkylidene geometric isomers *opposite* to those observed.

Turn next to Scheme V, the "short" D^- addition/elimination cycle. Again, an "anti" deuteride elimination from **1- α -d₁-k** (transition state XI utilizing rotamer VIIIc) affords the principal product, **2k**. No "syn" deuteride elimination, which would yield **2t**, occurs. This is in qualitative agreement with the calculations on $(\eta\text{-C}_5\text{H}_5)\text{Re}(\text{NO})(\text{PPh}_3)(\text{CH}_2\text{H}')$ ($\text{CH}' = \text{elongated CH bond}$), which indicated a slight bond weakening when H' was antiperiplanar to PPh_3 (Figure 6).

Consider the possibility of an anti *hydride* (H^-) abstraction in Scheme V. Such a reaction would have to occur via rotamer VIIIa (shown in Scheme IV) and would result in a product (**2t- α -d₁**) other than the one observed. However, as noted above, rotamer

VIIIa is significantly more stable than VIIIc. Therefore, if the "anti" elimination mechanism (transition state XI, Scheme VII) for hydride abstraction is correct, the *least stable rotamer of 1 is the most kinetically reactive one*.

We turn finally to Scheme IV, the "long" D^- addition/elimination cycle. It is again clear that only "anti" elimination can lead to the observed products. In each case, the least stable **1- α -d₁** rotamer (Vc, VIIIc) is the most reactive toward $\text{Ph}_3\text{C}^+\text{PF}_6^-$.

Hence we have formulated a mechanism for X^- group abstraction from $(\eta\text{-C}_5\text{H}_5)\text{Re}(\text{NO})(\text{PPh}_3)(\text{CHXR})$ alkyls that is consistent with all of the observed data. Are there others? We consider a variation in which electron transfer occurs (from Re to Ph_3C^+) prior to X loss to be likely. The Ph_3C^+ is of course very bulky, and the close approach to X shown in XI–XIV may not be realistic. Since our suggestion of this possibility,⁷ Cooper has obtained evidence for radical cation intermediates in the abstraction of α hydrides from $(\eta\text{-C}_5\text{H}_5)_2\text{W}(\text{CH}_3)_2$ by Ph_3C^+ .⁴¹ Also, distinctly different mechanisms might appear in time that equally well fit our observations. We have considered the possibility of Ph_3C^+ –nitrosyl coordination. While this would alter the relative sizes of the rhenium ligands, we do not presently see any reason why it would yield energetically more favorable reaction pathways or better explain our results.

At the present level of sophistication, our proposed mechanism does not address the reason *why* the least stable rotamer of **1** is the most reactive toward $\text{Ph}_3\text{C}^+\text{PF}_6^-$. If the kinetic product were **2t** instead of **2k**, "product development control" could be invoked. However, since the least stable rotamer affords the *less* stable of two possible isomeric products, there must be some unique means of transition-state stabilization available to **Vc** \rightarrow **2k- α -d₁** (and VIIIc \rightarrow **2k**) but not **Va** \rightarrow **2t** (and VIIIa \rightarrow **2t- α -d₁**).⁴² For instance, attractive interactions between $\eta\text{-C}_5\text{H}_5$ rings and neighboring phenyls have been previously observed crystallographically.⁴³ However, these are not in evidence in any of the X-ray structures (**2t-CHCl₂**, **5t-CH₂Cl₂**, (*-*)-**R-1**^{1b}) we have completed to date. Furthermore, aliphatic homologues of **1** behave similarly toward $\text{Ph}_3\text{C}^+\text{PF}_6^-$.⁷ While other systems have been found in which the less stable of two equilibrating species reacts more rapidly to give the less stable of two other equilibrating species,⁴⁴ we know of no example exactly analogous (nondissociative equilibria; Curtin–Hammett conditions;⁴² exclusive operation of one pathway) to the case in hand.

4. Concluding Remarks. This study has served to define many conceptual analogies between $\text{C}=\text{C}$ double bonds and $\text{Re}=\text{C}$ double bonds. However, rhenium, unlike carbon, can form a *fifth* bond and remain (pseudo) tetrahedral. This adds extra dimensions of structure and reactivity.

The ability of rhenium to form a fifth bond is critical to the excellent stereocontrol in the reaction of **1** with $\text{Ph}_3\text{C}^+\text{PF}_6^-$ and the reactions of **2t** and **2k** with nucleophiles. In aldehydes and ketones with *adjacent* chiral centers, nucleophilic attack upon the $>\text{C}=\text{O}$ bond (neither terminus of which is itself chiral) commonly occurs with 30–90% diastereoselectivity.⁴⁵ In the case of **2t** and

(41) Hayes, J. C.; Pearson, G. D. N.; Cooper, N. J. *J. Am. Chem. Soc.* **1981**, *103*, 4648.

(42) (a) This is most readily seen by superimposing two energy–reaction coordinate diagrams onto Figure 7. From Baird's data,²¹ it can be estimated that the Vc/VIIIc type rotamers are at most 1 kcal/mol higher in energy than the Va/VIIIa type rotamers. When energy curves connecting the former to **2k** and the latter to **2t** are drawn, the Curtin–Hammett principle^{42b-d} requires that the transition state leading to **2k** be placed at a *lower* position on the energy axis (Figure 7) than the transition state leading to **2t**. (b) Carey, F. A.; Sundberg, R. J. "Advanced Organic Chemistry. Part A: Structure and Mechanisms"; Plenum: New York, 1977; pp 168–170. (c) Seeman, J. I.; Sanders, E. B.; Farone, W. A. *Tetrahedron* **1980**, *36*, 1173. (d) Seeman, J. I. *Chem. Rev.*, in press.

(43) Brunner, H.; Agrifoglio, G.; Bernal, I.; Creswick, M. W. *Angew. Chem., Int. Ed. Engl.* **1980**, *19*, 641 and references therein. Bernal, I.; Creswick, M.; Brunner, H.; Agrifoglio, G. *J. Organomet. Chem.* **1980**, *198*, C4.

(44) Such behavior may be relatively common in homogeneous catalysis. For instance, the direct oxidative addition of H_2 to $\text{RhCl}(\text{PPh}_3)_3$ can occur, but addition of H_2 to $\text{RhCl}(\text{PPh}_3)_2$ (generated in small quantities by PPh_3 dissociation) is at least 10^4 times faster. Halpern, J.; Wong, C. S. *J. Chem. Soc., Chem. Commun.* **1973**, 629.

2k, the rhenium terminus of $\text{Re}=\text{C}$ is chiral, and diastereoselectivities of 90–100% are observed. Benzylidenes **2t** and **2k** have two principal elements of stereoisomerism: (i) a center of chirality; (ii) an unsymmetrically substituted multiple bond.⁴⁶ Conversion of **2t** and **2k** to **3–7** entails the stereospecific or stereoselective conversion of the second element⁴⁶ (which contains rhenium) to a new chiral center (which does not contain rhenium). The presence of large (PPh_3), medium (C_6H_5), and small (NO) ligands on rhenium, coupled with a strong rhenium–carbon π bond to lock the benzylidene geometry, provides a steric basis for the chirality transfer. There is a strong conceptual parallel to Cram's rule⁴⁵ and related models for asymmetric induction.^{37a}

While the reactions described herein do not provide a basis for new *catalytic* asymmetric syntheses, stoichiometric metal–carbon bond-cleavage reactions can be anticipated⁴⁷ to give chiral organic molecules such as $\text{C}_6\text{H}_5\text{CHDBr}$ and $\text{C}_6\text{H}_5\text{CHDT}$ in high optical yields. This topic will be the subject of future reports from our laboratory. We also emphasize the close interplay of theory and experiment that guided this work.⁴⁸ Additional predictions of extended Hückel MO calculations in organorhenium chemistry are presently under study.

Experimental Section

General Information. All reactions were conducted under an atmosphere of dry N_2 . Chromatographies were conducted in air unless noted. Hexanes were distilled from potassium metal, and CH_2Cl_2 was distilled from P_2O_5 . Benzene, CHCl_3 , and other solvents were commercial reagent grade and simply degassed with N_2 prior to use. CD_2Cl_2 and CD_3CN were degassed and distilled from P_2O_5 . Other deuterated solvents were used without purification unless noted.

IR spectra were recorded on a Perkin-Elmer Model 521 spectrometer. ^1H NMR and ^{13}C NMR spectra were (unless otherwise noted) recorded at ambient probe temperature on a Bruker WP-200 spectrometer at 200 and 50 MHz, respectively, and referenced to internal $(\text{CH}_3)_4\text{Si}$. UV-vis spectra were recorded on a Cary 219 spectrophotometer. Mass spectra were obtained on an AEI-M59 instrument. Melting points were recorded on a Büchi Schmeltpunktbestimmungsapparat and were not corrected. Microanalyses were conducted by Galbraith.

Starting Materials. $(\eta\text{-C}_5\text{H}_5)\text{Re}(\text{NO})(\text{PPh}_3)(\text{CH}_3)$ was prepared as previously described.^{15b} $\text{Ph}_3\text{C}^+\text{PF}_6^-$ was purchased from Aldrich and Columbia Organic Chemicals and stored under N_2 in the refrigerator. Over the course of these investigations the quality of the $\text{Ph}_3\text{C}^+\text{PF}_6^-$ varied considerably. It was found that recrystallization of $\text{Ph}_3\text{C}^+\text{PF}_6^-$ from CH_2Cl_2 /benzene or from CH_2Cl_2 /ether under N_2 gave pure $\text{Ph}_3\text{C}^+\text{PF}_6^-$ (50–60% recovery).⁴⁹ $\text{C}_6\text{H}_5\text{Li}$ (2 M in C_6H_6 /ether), $\text{Li}(\text{C}_2\text{H}_5)_3\text{BD}$ (1 M in THF), and $\text{CH}_3\text{CH}_2\text{MgBr}$ (3 M in Et_2O) were purchased from Aldrich; $\text{C}_6\text{H}_5\text{CH}_2\text{MgCl}$ (1.8 M in THF) and CH_3LiLiBr complex (1.4 M in THF) were purchased from Alfa. Except for the CH_3Li ,⁵⁰ these were used without standardization. PMe_3 was obtained from Strem Chemicals and used without purification.

Preparation of $(\eta\text{-C}_5\text{H}_5)\text{Re}(\text{NO})(\text{PPh}_3)(\text{CH}_2\text{C}_6\text{H}_5)$ (1**).** The following procedure is similar to the one developed by Wong and Tam.⁵¹ To a 100-mL Schlenk flask was added 0.517 g (0.926 mmol) of $(\eta\text{-C}_5\text{H}_5)\text{Re}(\text{NO})(\text{PPh}_3)(\text{CH}_3)$ and 50 mL of CH_2Cl_2 . The resulting orange solution was then cooled to -78°C , and 0.396 g (1.020 mmol) of $\text{Ph}_3\text{C}^+\text{PF}_6^-$ was added as a solid. After the reaction mixture was stirred for 30 min at -78°C (during which time a yellow solution formed), 0.700 mL of $\text{C}_6\text{H}_5\text{Li}$ (2 M in benzene/ether) was added dropwise. The reaction mixture was stirred at -78°C for an additional 15 min and then allowed to warm to room temperature. The solvent was then removed by rotary evaporation. The residue was taken up in benzene and filtered through a 2-in. silica gel plug. The benzene was removed by rotary evaporation to give an orange solid. Overnight recrystallization from CH_2Cl_2 /hexanes in a freezer gave fine orange crystals of **1**, which were collected by filtration, washed with hexanes, and dried (0.483 g, 0.761 mmol, 82%); mp $180\text{--}182^\circ\text{C}$; ^{13}C NMR (ppm, CDCl_3) 90.56, -3.94 (d, $J_{13\text{C}-31\text{P}} = 4.8$

Hz), phenyl carbons at 133.68 (d, $J_{13\text{C}-31\text{P}} = 9.7$ Hz), 130.07 (d, $J = 3.2$ Hz), 128.41 (d, $J = 9.7$ Hz), 127.61, 127.23, 121.90, ipso phenyl carbons not observed; other data.⁵¹ IR (cm^{-1} , CH_2Cl_2) $\nu_{\text{N=O}}$ 1626 s; ^1H NMR (CDCl_3) δ 7.09–7.49 (m, 20 H), 4.74 (d, $J_{1\text{H}-31\text{P}} = 1.0$ Hz, 5 H), 3.50 (dd, $J_{1\text{H}-1\text{H}} = 11.8$ Hz, $J_{1\text{H}-31\text{P}} = 7.9$ Hz, 1 H), 2.89 (dd, $J_{1\text{H}-1\text{H}} = 11.8$ Hz, $J_{1\text{H}-31\text{P}} = 2.8$ Hz, 1 H). Anal. Calcd for $\text{C}_{30}\text{H}_{27}\text{NOPRe}$: C, 56.67; H, 4.29; N, 2.21; P, 4.88. Found: C, 56.84; H, 4.32; N, 2.14; P, 5.06.

Preparation of $ac\text{-}[(\eta\text{-C}_5\text{H}_5)\text{Re}(\text{NO})(\text{PPh}_3)(=\text{CHC}_6\text{H}_5)]^+\text{PF}_6^-$ (2t**).** To a 100-mL Schlenk flask was added 0.302 g (0.477 mmol) of $(\eta\text{-C}_5\text{H}_5)\text{Re}(\text{NO})(\text{PPh}_3)(\text{CH}_2\text{C}_6\text{H}_5)$ (**1**) and 30 mL of CH_2Cl_2 . The resulting orange solution was cooled to -78°C and 0.203 g (0.524 mmol) of $\text{Ph}_3\text{C}^+\text{PF}_6^-$ was added as a solid. The resulting yellow solution was stirred at -78°C for 30 min and then allowed to warm to room temperature. After an additional 2 h, hexanes (20 mL) were added (to inhibit oiling upon concentration), and both solvents were removed under an oil pump vacuum. The resulting solid was washed with hexanes and then small portions of ether. An off-yellow powder was obtained. Recrystallization from CH_2Cl_2 /hexanes (freezer) gave 0.278 g (0.358 mmol, 75%) of **2t** as a yellow powder, mp $225\text{--}230^\circ\text{C}$ dec. Alternatively, diffusion of petroleum ether (bp $30\text{--}60^\circ\text{C}$) into a CHCl_3 solution of **2t** afforded bright yellow crystals of the monosolvate **2t**· CHCl_3 (0.312 g, 0.348 mmol, 73%); mp 215°C dec; ^1H NMR (CDCl_3) δ 15.30 (s, 1 H), 7.52–7.18 (m, 20 H), 6.06 (s, 5 H); ^{13}C NMR (ppm, CDCl_3) 288.6 (Re=C), phenyl carbons at 151.8, 133.9, 133.0 (d, $J_{13\text{C}-31\text{P}} = 11.9$ Hz), 132.2, 131.9, 129.5 (d, $J_{13\text{C}-31\text{P}} = 10.2$ Hz), 129.1, 127.9 (ipso PPh_3 carbons, portion of doublet with other portion likely obscured by 129.1-ppm resonance), C_5H_5 at 99.6; ^{13}C NMR (CD_2Cl_2 , in situ, for comparison to **2k** chemical shifts below) 287.4, 100.0; IR (cm^{-1} , CH_2Cl_2) $\nu_{\text{N=O}}$ 1708 s.

Preparation of $sc\text{-}[(\eta\text{-C}_5\text{H}_5)\text{Re}(\text{NO})(\text{PPh}_3)(=\text{CHC}_6\text{H}_5)]^+\text{PF}_6^-$ (2k**).** Preparative-scale syntheses of **2k** were conducted as described above for **2t**. In each case, solutions were stirred for 0.5 h at -78°C before reaction. Spectroscopic-scale syntheses were conducted at -78°C as described before for the isomerization rate measurements. ^1H NMR (CD_2Cl_2) δ 16.08 (s, 1 H), 7.52–7.18 (m, 20 H), 5.89 (s, 5 H); ^{13}C NMR (ppm, CD_2Cl_2 , -63°C) 280.5, 98.5, phenyl carbons obscured by Ph_3CH .

Photolysis of **2t.** The following experiment is representative: To a septum-capped 5-mm NMR tube was added **2t** (0.0290 g, 0.0370 mmol), *p*-di-*tert*-butylbenzene standard (0.0022 g, 0.012 mmol), and acetone- d_6 (dried over 4A molecular sieves). The tube was then subjected to five freeze-pump-thaw degassing cycles, and a ^1H NMR spectrum (including integrals of the **2t** and standard resonances) was recorded. The tube was then placed in a large Pyrex test tube partially filled with acetone and the test tube in turn placed in a large unsilvered Pyrex Dewar containing a dry ice/acetone cooling bath. A Hanovia 450-W lamp was suspended in a quartz immersion well and placed adjacent to the Dewar such that ca. 5 cm separated the lamp from the sample. After 3 h of irradiation at -78°C , the NMR tube was transferred to a Varian T-60 spectrometer (ambient probe temperature; previously tuned to **2t** in acetone- d_6) and five spectra of the C_5H_5 region (**2t**, δ 6.42; **2k**, δ 6.30) were recorded in rapid succession (negligible isomerization; see Table II). The relative integrals were averaged and indicated a $(57 \pm 1):(43 \pm 1)$ **2t**/**2k** ratio. The sample was allowed to stand overnight at room temperature in the dark. Integration of the **2t** vs. *p*-di-*tert*-butylbenzene resonances indicated $>95\%$ of the original **2t** to be present.

Rates of Isomerization: **2k \rightarrow **2t**.** To a septum-capped NMR tube was added 0.0148–0.0168 g of $(\eta\text{-C}_5\text{H}_5)\text{Re}(\text{NO})(\text{PPh}_3)(\text{CH}_2\text{C}_6\text{H}_5)$ (**1**) in 0.300 mL of CD_2Cl_2 . The NMR tube was then cooled to the temperature of data collection (Table II), whereupon 1.2 equiv of $\text{Ph}_3\text{C}^+\text{PF}_6^-$ in 0.200 mL of CD_2Cl_2 was added via gas-tight syringe. The NMR tube was then quickly transferred to a NMR probe that had been preequilibrated to the appropriate temperature. Disappearance of **2k** was monitored by integration of the δ 16.08 resonance. Standard ln (integral) vs. time plots yielded the data in Table II. ΔH^\ddagger and ΔS^\ddagger were obtained from ln (k_{obsd}/T) vs. $1/T$ plots.

Preparation of $(SS,RR)\text{-}(\eta\text{-C}_5\text{H}_5)\text{Re}(\text{NO})(\text{PPh}_3)(\text{CHDC}_6\text{H}_5)$ (1- α -d₁-t**).** Benzylidene **2t** (0.154 g, 0.198 mmol) was dissolved in 20 mL of CH_2Cl_2 in a 100-mL Schlenk flask and cooled to -78°C . Then 0.220 mL (0.220 mmol) of $\text{Li}(\text{C}_2\text{H}_5)_3\text{BD}$ (1.0 M in THF) was added dropwise. The solution was allowed to warm to room temperature and the solvent removed under oil pump vacuum. The resulting orange residue was extracted with benzene and filtered through a 2-in. silica gel plug. The benzene was removed and the residue recrystallized from CH_2Cl_2 /hexanes to give **1- α -d₁-t** as an orange solid (0.116 g, 0.183 mmol, 92%), mp $220\text{--}222^\circ\text{C}$ dec. Spectral data: Tables III and VI.

Preparation of $(SR,RS)\text{-}(\eta\text{-C}_5\text{H}_5)\text{Re}(\text{NO})(\text{PPh}_3)(\text{CHDC}_6\text{H}_5)$ (1- α -d₁-k**).** A. To a -78°C solution of **2k** (prepared from 0.187 mmol of **1** as described above) was added dropwise 0.280 mL of $\text{Li}(\text{C}_2\text{H}_5)_3\text{BD}$ (1.0 M in THF). After 15 min at -78°C , the reaction was allowed to warm to room temperature while solvent was simultaneously removed under oil

(45) (a) Cram, D. J.; Abd Elhafey, F. A. J. Am. Chem. Soc. 1952, 74, 5828. (b) Morrison, J. D.; Mosher, H. S. "Asymmetric Organic Reactions"; American Chemical Society: Washington, D.C., 1976, Chapter 3.

(46) According to some conventions, the $\text{Re}=\text{C}$ bond defines a plane of chirality: Lemière, G. L.; Alderweifel, F. C. J. Org. Chem. 1980, 45, 4175.

(47) Flood, T. C. Top. Stereochem. 1981, 12, 37.

(48) Hoffmann, R. Science (Washington, D.C.) 1981, 211, 995.

(49) Patton, A. T.; UCLA, unpublished procedure.

(50) Lipton, M. F.; Sorensen, C. M.; Sadler, A. C.; Shapiro, R. H. J. Organomet. Chem. 1980, 186, 155.

(51) (a) Wong, W.-K.; Tam, W.; Gladysz, J. A. J. Am. Chem. Soc. 1979, 101, 5440. (b) Tam, W. Ph.D. Thesis, UCLA, Los Angeles, CA, 1979.

Table VI. Summary of 16-eV Mass Spectral Data

complex	ions, m/e for ^{187}Re (% of base peak)				
	M^+	$\text{M}^+ - \text{R}$	$\text{M}^+ - \text{PPh}_3$	PPh_3^+	other
1- α - d_1 -t	636 (47.8)	544 (100)	374 (20.9)	262 (41.5)	
1- α - d_1 -k	636 (40.4)	544 (100)	374 (27.3)	262 (62.3)	
3t	649 (6.4)	544 (73.5)	387 (25.8)	262 (100)	359 (13.8)
3k	649 (5.7)	544 (72.1)	387 (29.2)	262 (100)	359 (11.5)
4t	663 (6.8)	544 (82.1)	401 (21.4)	262 (100)	359 (14.4)
4k	663 (9.2)	544 (100)	401 (6.6)	262 (12.1)	359 (27.1)
5t	not observed ^a	544 (29.9)	463 (28.7)	262 (100)	634 ^b (1.2) 359 (40.5) 634 ^b (6.5) 359 (29.5)
5k	725 (3.9)	544 (51.1)	463 (28.1)	262 (100)	634 ^b (6.5) 359 (29.5)
7t	665 (1.1)	544 (100)	not observed	262 (81.1)	635 ^c (21.7) 373 (14.3)

^a The absence of a M^+ ion for 5t but not 5k may be a consequence of the different probe temperatures used: 5t, 210 °C; 5k, 190 °C. ^b $\text{M}^+ = \text{CH}_2\text{C}_6\text{H}_5$. ^c $\text{M}^+ = \text{NO}$.

pump vacuum. The residue was extracted with benzene and filtered through a 2-in. silica gel plug. The benzene was removed by rotary evaporation and the orange solid ^1H NMR assayed. Integration of the $\text{ReCHDC}_6\text{H}_5$ resonances indicated a $(92 \pm 2):(8 \pm 2)$ ratio of 1- α - d_1 -k to 1- α - d_1 -t. Recrystallization from CH_2Cl_2 /hexanes gave 0.096 g (0.151 mmol, 80%) of (predominantly) 1- α - d_1 -k.

B. Diastereomerically pure 1- α - d_1 -k was prepared by the reaction of $\text{Li}(\text{C}_2\text{H}_5)_3\text{BH}$ with 2t- α - d_1 (preparation below) in a procedure analogous to the one above for 1- α - d_1 -t. Spectral data are given in Tables III and VI.

Preparation of $(\text{SS},\text{RR})-(\eta\text{-C}_5\text{H}_5)\text{Re}(\text{NO})(\text{PPh}_3)(\text{CH}(\text{CH}_3)\text{C}_6\text{H}_5)$ (3t). Benzylidene 2t (0.306 g, 0.393 mmol) was dissolved in 40 mL of CH_2Cl_2 in a Schlenk flask and cooled to -78°C . Then 0.320 mL of CH_3Li (1.4 M in ether) was added dropwise. The solution turned orange and was allowed to warm to room temperature. Solvent was removed under oil pump vacuum. The resulting residue was extracted with benzene and filtered through a 2-in. silica gel plug. The benzene was removed by rotary evaporation, and the orange solid that remained was chromatographed on a 13×2.5 cm silica gel column (1:1 CH_2Cl_2 /hexanes). The orange band was collected, and solvent was removed under oil pump vacuum to give 0.214 g (0.330 mmol, 84%) of 3t as an orange powder, mp 237–240 °C dec. Spectroscopic data are given in Tables III and VI.

Preparation of $(\text{SS},\text{RR})-(\eta\text{-C}_5\text{H}_5)\text{Re}(\text{NO})(\text{PPh}_3)(\text{CH}(\text{CH}_2\text{CH}_3)\text{C}_6\text{H}_5)$ (4t). Benzylidene 2t (0.105 g, 0.135 mmol) was dissolved in 20 mL of CH_2Cl_2 in a Schlenk flask and cooled to -78°C . Then 0.180 mL of $\text{CH}_3\text{CH}_2\text{MgBr}$ (3 M in THF) was added dropwise. After 15 min at -78°C , the reaction was allowed to warm to room temperature while solvent was simultaneously removed under oil pump vacuum. The residue was extracted with benzene and filtered through a 2-in. silica gel plug. The benzene was removed by rotary evaporation, and the resulting orange oil was chromatographed on a 13×2.5 cm silica gel column (1:1 CH_2Cl_2 /hexanes). The orange band was collected, and solvent was removed under oil pump vacuum to give 0.078 g (0.118 mmol, 87%) of 4t as an orange powder, mp 183–185 °C dec. Spectroscopic data are given in Tables III and VI.

Preparation of $(\text{SS},\text{RR})-(\eta\text{-C}_5\text{H}_5)\text{Re}(\text{NO})(\text{PPh}_3)(\text{CH}(\text{CH}_2\text{C}_6\text{H}_5)\text{C}_6\text{H}_5)$ (5t). Benzylidene 2t (0.309 g, 0.397 mmol) was dissolved in 40 mL of CH_2Cl_2 in a Schlenk flask and cooled to -78°C . Then 0.330 mL of $\text{C}_6\text{H}_5\text{CH}_2\text{MgCl}$ (1.8 M in THF) was added dropwise. After 20 min at -78°C , the reaction was allowed to warm to room temperature while solvent was simultaneously removed under oil pump vacuum. The residue was extracted with benzene and filtered through a 2-in. silica gel plug. The benzene was removed by rotary evaporation, and the resulting orange oil was chromatographed on a 13×2.5 cm silica gel column (1:1 CH_2Cl_2 /hexanes). The orange band was collected, and solvent was removed under oil pump vacuum to give 0.259 g (0.358

mmol, 90%) of 5t as an orange powder, mp 222–225 °C dec. Spectroscopic data are given in Tables III and VI.

Preparation of $(\text{SR},\text{RS})-(\eta\text{-C}_5\text{H}_5)\text{Re}(\text{NO})(\text{PPh}_3)(\text{CH}(\text{PMe}_3)\text{C}_6\text{H}_5)]^+\text{PF}_6^-$ (6t). Benzylidene 2t (0.116 g, 0.149 mmol) was dissolved in 20 mL of CH_2Cl_2 in a Schlenk flask and cooled to -78°C . Then 0.030 mL (0.022 g, 0.295 mmol) of PMe_3 was added. The resulting orange solution was stirred for 5 min at -78°C . The reaction was then allowed to warm to room temperature while solvent was simultaneously removed under oil pump vacuum.⁵² The resulting solid was taken up in CH_2Cl_2 ; hexanes were then layered onto this solution. On standing, orange needles of 6t formed. These were collected by filtration and dried (0.105 g, 0.123 mmol, 82%), mp 229–230 °C dec. Spectroscopic data are given in Table III.

Preparation of $(\text{SR},\text{RS})-(\eta\text{-C}_5\text{H}_5)\text{Re}(\text{NO})(\text{PPh}_3)(\text{CH}(\text{OCH}_3)\text{C}_6\text{H}_5)$ (7t). To a solution of 1 (0.385 g, 0.609 mmol) in dry CH_2Cl_2 (30 mL) at -78°C was added solid $\text{Ph}_3\text{C}^+\text{PF}_6^-$ (0.334 g, 0.861 mmol). The resulting mixture was stirred for 30 min and then allowed to warm to room temperature. After 4 h at room temperature, a CH_3ONa solution prepared from Na (0.64 g, 27.8 mmol) and anhydrous CH_3OH (15 mL) was added. The resulting mixture was stirred for 20 min, whereupon the solvent was removed under reduced pressure. The residue was extracted with CH_2Cl_2 ⁵² and recrystallized from CH_2Cl_2 /hexanes to give yellow crystals of 7t (0.299 g, 0.452 mmol, 74%), mp 169–172 °C dec. Spectroscopic data are given in Tables III and VI. Anal. Calcd for $\text{C}_{31}\text{H}_{29}\text{NO}_2\text{PRe}$: C, 56.01; H, 4.40; N, 2.11; P, 4.66. Found: C, 55.81; H, 4.47; N, 2.34; P, 4.61.

Preparation of $(\text{SR},\text{RS})-(\eta\text{-C}_5\text{H}_5)\text{Re}(\text{NO})(\text{PPh}_3)(\text{CH}(\text{CH}_3)\text{C}_6\text{H}_5)$ (3k). To a -78°C solution of 2k (prepared from 0.160 mmol of 1 as described above) was added dropwise 0.350 mL of CH_3Li (1.4 M in ether). After 5 min at -78°C (during which time the solution turned from yellow to orange), the reaction was allowed to warm to room temperature while solvent was simultaneously removed under oil pump vacuum. The residue was extracted with benzene/ CH_2Cl_2 (1:1) and filtered through a 2-in. silica gel plug. The solvent was removed and the residue chromatographed on a 13×2.5 cm silica gel column (1:1 CH_2Cl_2 /hexanes). The orange band was collected. Solvent removal afforded an orange powder (0.0893 g, 0.138 mmol, 86%), mp 186–188 °C dec, which was shown by ^1H NMR (C_5H_5 resonances) to be a $(94 \pm 1):(6 \pm 1)$ 3k/3t mixture.⁵³ Spectroscopic data are given in Tables III and VI.

Preparation of $(\text{SR},\text{RS})-(\eta\text{-C}_5\text{H}_5)\text{Re}(\text{NO})(\text{PPh}_3)(\text{CH}(\text{CH}_2\text{CH}_3)\text{C}_6\text{H}_5)$ (4k). To a -78°C solution of 2k (prepared from 0.300 mmol of 1 as described above) was added dropwise 0.400 mL of $\text{CH}_3\text{CH}_2\text{MgBr}$ (3.0 M in ether). After 5 min at -78°C , the reaction was allowed to warm to room temperature while solvent was simultaneously removed under oil pump vacuum. The residue was extracted with benzene and filtered through a 2-in. silica gel plug in a glovebox. The benzene was removed under oil pump vacuum, and the resulting residue was chromatographed on a 13×2.5 cm silica gel column (1:1 CH_2Cl_2 /hexanes). The orange band was collected. Solvent removal afforded an orange powder (0.100 g, 0.150 mmol, 50%), mp 172–175 °C dec, which was shown by ^1H NMR (C_5H_5 resonances) to be a $(94 \pm 1):(6 \pm 1)$ 4k/4t mixture.⁵³ Spectroscopic data are given in Tables III and VI.

Preparation of $(\text{SR},\text{RS})-(\eta\text{-C}_5\text{H}_5)\text{Re}(\text{NO})(\text{PPh}_3)(\text{CH}(\text{CH}_2\text{C}_6\text{H}_5)\text{C}_6\text{H}_5)$ (5k). To a -78°C solution of 2k (prepared from 0.160 mmol of 1 as described above) was added dropwise 0.180 mL of $\text{C}_6\text{H}_5\text{CH}_2\text{MgCl}$ (1.8 M in THF). After 15 min at -78°C , the reaction was allowed to warm to room temperature while solvent was simultaneously removed under oil pump vacuum. The residue was extracted with benzene and filtered through a 2-in. silica gel plug in a glovebox. The benzene was removed under oil pump vacuum, and the resulting oil was chromatographed on a 13×2.5 cm silica gel column (1:1 CH_2Cl_2 /hexanes). The orange band was collected. Solvent removal afforded an orange powder (0.095 g, 0.132 mmol, 82%), mp 194–197 °C dec, which was shown by ^1H NMR (C_5H_5 resonances) to be a $(94 \pm 1):(6 \pm 1)$ 5k/5t mixture.⁵³ Spectroscopic data are given in Tables III and VI.

Preparation of $(\text{SS},\text{RR})-(\eta\text{-C}_5\text{H}_5)\text{Re}(\text{NO})(\text{PPh}_3)(\text{CH}(\text{PMe}_3)\text{C}_6\text{H}_5)]^+\text{PF}_6^-$ (6k). To a -78°C solution of 2k (prepared from 0.165 mmol of 1 as described above) was added 0.020 mL (0.014 g, 0.197 mmol) of PMe_3 . After 15 min at -78°C , the reaction was allowed to warm to room temperature while solvent was simultaneously removed under oil pump vacuum. The residue was taken up in CH_2Cl_2 . Dia-

(52) ^1H NMR analysis was conducted at this stage to assay diastereomer purity. All t isomers were $\geq 99\%$ pure.

(53) Recrystallization of this mixture from CH_2Cl_2 /hexanes over the course of several days in the freeze afforded pure k isomer. For 3k, it was necessary to halt the crystallization after 10–20% recovery in order to prevent cocrystallization of 3t.

stereomerically pure **6k** was obtained as an orange powder (0.099 g, 0.116 mmol, 70%), mp 122–123 °C dec, by allowing ether to slowly diffuse into this solution in a freezer. Spectroscopic data are given in Table III.

An ^1H NMR monitored experiment (see isomerization rate studies) was conducted on a 0.024 mmol scale in CD_2Cl_2 at -78°C . Addition of 0.005 mL (0.049 mmol) of PMe_3 to **2k** gave an orange solution, which upon warming to room temperature was shown by integration of the C_5H_5 resonances to be a $(94 \pm 1):(6 \pm 1)$ **6k/6t** mixture.

Preparation of (SS,RR)- $(\eta\text{-C}_5\text{H}_5)\text{Re}(\text{NO})(\text{PPh}_3)(\text{CH}(\text{OCH}_3)\text{C}_6\text{H}_5)$ (7k**).** To a -78°C solution of **2k** (prepared from 0.350 mmol of **1** as described above) was added a solution of CH_3ONa generated from Na (0.20 g, 8.7 mmol) and anhydrous CH_3OH (8 mL). After 10 min at -78°C , the reaction was allowed to warm to room temperature while solvent was simultaneously removed under oil pump vacuum. The resulting residue was extracted with benzene (ca. 200 mL) and dried over MgSO_4 . Solvent was removed from the filtrate; ^1H NMR analysis of the residue indicated a $(78 \pm 1):(22 \pm 1)$ **7k/7t** ratio. Diffusion recrystallization of the residue from CH_2Cl_2 /hexanes in the freezer gave orange prisms (0.079 g, 0.119 mmol, 35%), which were shown by ^1H NMR (C_5H_5 resonances) to be a $(90 \pm 1):(10 \pm 1)$ **7k/7t** mixture, mp 155–172 °C dec.⁵³ Spectroscopic data are given in Table III. Anal. Calcd for $\text{C}_{31}\text{H}_{29}\text{NO}_2\text{PRe}$: C, 56.01; H, 4.40. Found: C, 55.93; H, 4.51.

A ^1H NMR monitored experiment (see isomerization rate studies) was conducted on a 0.019 mmol scale in CD_2Cl_2 at -78°C . A CD_3ONa solution that was generated from Na (0.018 g, 0.782 mmol) and CD_3OD (0.300 mL) was added to **2k**. Reaction was complete within 3 min as assayed by a ^1H NMR spectrum at -70°C . A $(85 \pm 1):(15 \pm 1)$ **7k-d₃/7t-d₃** mixture formed.

Reaction of 1- α -d₁-t with $\text{Ph}_3\text{C}^+\text{PF}_6^-$. Preparation of 2t- α -d₁. To a 100-mL Schlenk flask were added 0.211 g (0.332 mmol) of 1- α -d₁-t and 20 mL of CH_2Cl_2 . The resulting solution was cooled to -78°C , and 0.135 g (0.349 mmol) of $\text{Ph}_3\text{C}^+\text{PF}_6^-$ was added as a solid. The resulting yellow solution was stirred at -78°C for 30 min and then allowed to warm to room temperature. After an additional 30 min, solvent was removed under oil pump vacuum. The residue was extracted with hexanes to recover the triphenylmethane. The hexanes were removed from the extracts via rotary evaporation, and the residue was recrystallized from hot 95% ethanol. Fluffy white crystals of triphenylmethane (0.059 g, 0.241 mmol, 73%) were obtained. Analysis of the m/e 244:245 peak ratio in the 16-eV mass spectrum (including comparison to an authentic sample) indicated a natural abundance $\text{Ph}_3\text{CH}/\text{Ph}_3\text{CD}$ ratio.

The residue remaining after hexane extraction was taken up in CH_2Cl_2 and filtered through a 2-in. silica gel plug. The CH_2Cl_2 was then removed by rotary evaporation, and the residue was diffusion recrystallized from CHCl_3 /petroleum ether (bp 35–60 °C). Yellow prisms of 2t- α -d₁- CHCl_3 formed, which were collected by filtration and dried (0.195 g, 0.217 mmol, 65%; mp 215 °C, dec).⁵⁴

A ^1H NMR monitored reaction in CD_2Cl_2 was conducted analogously to the immediately following experiment and showed the sequential formation of **2k- α -d₁** (δ 5.89) and **2t- α -d₁** (δ 6.08).

Reaction of 1- α -d₁-k with $\text{Ph}_3\text{C}^+\text{PF}_6^-$. To a septum-capped NMR tube was added 0.020 g (0.032 mmol) of diastereomerically pure 1- α -d₁-k in 0.400 mL of CD_2Cl_2 . The tube was then cooled to -78°C , whereupon 0.0134 g (0.035 mmol) of $\text{Ph}_3\text{C}^+\text{PF}_6^-$ in 0.150 mL of CD_2Cl_2 was added via gas-tight syringe. The tube was quickly transferred to a -73°C NMR probe. A spectrum indicated the complete consumption of 1- α -d₁-k and the presence of **2k** (δ 16.08, 5.89) and some Ph_3CH (δ 5.59). Upon warming to room temperature in the NMR probe, **2k** disappeared as **2t** appeared. After several hours at room temperature, the $^*\text{Re}=\text{CHC}_6\text{H}_5$ (δ 15.30) and C_5H_5 (δ 6.05) resonances of **2t** were integrated repeatedly. From these data, a $(92 \pm 2):(8 \pm 2)$ ratio of **2t- α -d₀/2t- α -d₁** was calculated.

The contents of the NMR tube were applied to a preparative silica gel TLC plate, which was then eluted with 90:10 ethyl acetate/hexanes. The UV-active triphenylmethane band ($R_f \sim 0.7$) was isolated and extracted with CH_2Cl_2 . The eluent was concentrated to a residue, which was then recrystallized from hot 95% ethanol to give pure triphenylmethane. Analysis of the m/e 244:245 peak ratio in the 16 eV mass spectrum indicated a $(89 \pm 1):(11 \pm 1)$ $\text{Ph}_3\text{CD}/\text{Ph}_3\text{CH}$ ratio. The origin of the TLC plate was extracted with CH_2Cl_2 . The extract was concentrated to a residue, which was then diffusion recrystallized from CHCl_3 /petroleum ether (bp 35–60 °C). Yellow crystals of **2t-CHCl₃** (0.017 g,

0.019 mmol, 59%) were obtained. The **2t- α -d₁** content was assayed as described in the preceding paragraph (with identical results).

Reaction of 7t with $\text{Ph}_3\text{C}^+\text{PF}_6^-$. To a septum-capped NMR tube was added 0.016 g (0.024 mmol) of **7t** in 0.300 mL of CD_2Cl_2 . The tube was then cooled to -78°C , whereupon 0.010 g (0.025 mmol) of $\text{Ph}_3\text{C}^+\text{PF}_6^-$ in 0.140 mL of CD_2Cl_2 was added via gas-tight syringe. The tube was quickly transferred to a -65°C NMR probe. A ^1H NMR spectrum indicated the exclusive formation of **2t** and Ph_3COCH_3 (δ 2.91). A small amount of starting **7t** remained. No products derived via hydride abstraction from **7t** formed. A small resonance at ca. δ 3.3 was tentatively assigned to CH_3OCH_3 byproduct.

Reaction of 7k with $\text{Ph}_3\text{C}^+\text{PF}_6^-$. To a septum-capped ^1H NMR tube was added 0.020 g (0.030 mmol) of a 90:10 **7k/7t** mixture in 0.300 mL of CD_2Cl_2 . The tube was then cooled to -78°C , whereupon 0.018 g (0.046 mmol) of $\text{Ph}_3\text{C}^+\text{PF}_6^-$ in 0.150 mL of CD_2Cl_2 was added via gas-tight syringe. The tube was quickly transferred to a -70°C NMR probe. A ^1H NMR spectrum indicated the formation of a $(90 \pm 1):(10 \pm 1)$ ratio of **2k/2t** and Ph_3COCH_3 (δ 2.91). No other organometallic products were present; a very small δ 3.3 resonance was noted.

Calculations. All calculations were of the extended Hückel type,⁵⁵ with a weighted H_{ij} formula.⁵⁶ The ligand geometry about rhenium was assumed to be octahedral, and the following distances (Å) were used as input: Re–C, 2.10; Re–N, 1.78; N–O, 1.19; Re–P, 2.36; Re– C_5H_5 (distance to carbon), 2.33; C–C (C_5H_5), 1.40; C–H, 1.09; P–H, 1.44. Standard parameters were employed for carbon, nitrogen, oxygen, and hydrogen.⁵⁵ Those utilized for the other atoms were as follows: Re 6s, $H_{ii} = -9.36$ eV, $\zeta = 2.398$; Re 6p, $H_{ii} = -5.96$ eV, $\zeta = 2.372$; Re 5d, $H_{ii} = -12.66$ eV, $\zeta = 5.343$ (coefficient = 0.6359) and 2.277 (coefficient = 0.5677); P 3s, $H_{ii} = -18.6$ eV, $\zeta = 1.6$; P 3p, $H_{ii} = -14$ eV, $\zeta = 1.6$. The model nucleophile, H^- , was given $H_{ii} = -10$ eV and $\zeta = 1.3$.

Acknowledgment. This investigation was supported at UCLA by the Department of Energy (alkylidene synthesis) and the NIH (GM 29026-01; asymmetric induction) and at the University of Michigan by the donors of the Petroleum Research Fund, administered by the American Chemical Society. We warmly thank Professor Roald Hoffmann (Cornell University) for his interest in this study and several stimulating discussions. Helpful suggestions from Professors F. A. L. Anet and D. J. Cram, Dr. C. B. Knobler, and A. T. Patton (UCLA) are also gratefully acknowledged. Crystal structure determinations and FT NMR measurements made use of equipment obtained via NSF Departmental instrumentation grants. W.A.K. thanks the Regents of the University of California for a Fellowship.

Registry No. 1, 71763-28-5; 1- α -d₁-k, 82399-52-8; 1- α -d₁-t, 82399-53-9; **2k**, 74540-78-6; **2t**, 74561-64-1; **3k**, 82374-39-8; **3t**, 82399-54-0; **4k**, 82374-40-1; **4t**, 82399-55-1; **5k**, 82374-41-2; **5t**, 82399-56-2; **6k**, 82374-43-4; **6t**, 82399-58-4; **7k**, 76821-65-3; **7t**, 76770-56-4.

Supplementary Material Available: Figure 8, numbering of atoms in $ac\text{-}[(\eta\text{-C}_5\text{H}_5)\text{Re}(\text{NO})(\text{PPh}_3)(=\text{CHC}_6\text{H}_5)]^+\text{PF}_6^-\text{CHCl}_3$ (**2t-CHCl₃**); Figure 9, crystal packing diagram of **2t-CHCl₃** as viewed down axis A; Table VII, summary of crystallographic data for **2t-CHCl₃**; Table VIII, bond and short interatomic distances in **2t-CHCl₃**; Table IX, bond angles in **2t-CHCl₃**; Table X, atomic coordinates of **2t-CHCl₃** (atoms refined isotropically); Table XI, atomic coordinates of **2t-CHCl₃** (atoms refined anisotropically); Table XII, calculated and observed structure factors for **2t-CHCl₃**; Figure 10, numbering of atoms in $(SS,RR)\text{-}(\eta\text{-C}_5\text{H}_5)\text{Re}(\text{NO})(\text{PPh}_3)(\text{CH}(\text{CH}_2\text{C}_6\text{H}_5)\text{C}_6\text{H}_5)\text{-CH}_2\text{Cl}_2$ (**5t-CH₂Cl₂**); Figure 11, crystal packing diagram of **5t-CH₂Cl₂** as viewed down axis A; Table XIII, summary of crystallographic data for **5t-CH₂Cl₂**; Table XIV, bond and short interatomic distances in **5t-CH₂Cl₂**; Table XV, bond angles in **5t-CH₂Cl₂**; Table XVI, atomic coordinates of **5t-CH₂Cl₂** (atoms refined isotropically); Table XVII, atomic coordinates of **5t-CH₂Cl₂** (atoms refined anisotropically); Table XVIII, calculated and observed structure factors for **5t-CH₂Cl₂** (65 pages). Ordering information is given on any current masthead page.

(54) It should be noted that the sequence $(\eta\text{-C}_5\text{H}_5)\text{Re}(\text{NO})(\text{PPh}_3)(\text{CD}_3)^{7,15b} \rightarrow 1\text{-}\alpha\text{-d}_2 \rightarrow [2\text{k-}\alpha\text{-d}_1] \rightarrow 2\text{t-}\alpha\text{-d}_1$ (all by procedures analogous to those given for unlabeled compounds above) constitutes a considerably easier and more direct synthesis of **2t- α -d₁**.

(55) Hoffmann, R. *J. Chem. Phys.* **1963**, *39*, 1397. Hoffmann, R.; Lipscomb, W. N. *Ibid.* **1962**, *36*, 2179; **1962**, *37*, 2872.

(56) Ammeter, J. H.; Bürgi, H. B.; Thibault, J. C.; Hoffmann, R. *J. Am. Chem. Soc.* **1978**, *100*, 3686.